Hedging Cryptos with Bitcoin Futures

Francis Liu*

Natalie Packham†

Meng-Jou Lu ‡

Wolfgang Karl Härdle§¶

This version: December 2, 2022

Abstract

The introduction of derivatives on Bitcoin enables investors to hedge risk exposures in cryptocurrencies. Because of volatility swings and jumps in cryptocurrency prices, the traditional variance-based approach to obtain hedge ratios is infeasible. As a consequence, we consider two extensions of the traditional approach: first, different dependence structures are modelled by different copulae, such as the Gaussian, Student-t, Normal Inverse Gaussian and Archimedean copulae; second, different risk measures, such as value-at-risk, expected shortfall and spectral risk measures are employed to find the optimal hedge ratio. Extensive out-of-sample tests in the time period December 2017 until May 2021 give insights in the practice of hedging various cryptos and crypto indices, including Bitcoin, Ethereum, Cardano, the CRIX index and a number of crypto-portfolios. Evidence shows that BTC futures can effectively hedge BTC and BTC-involved indices. This promising result is consistent across different risk measures and copulae except for the Frank copula. On the other hand, we observe complex and diverse dependence structures between non-BTC-related cryptoassets and the BTC futures. As a consequence, the hedge performance of non-BTC-related cryptoassets is mixed and even infeasible for some assets.

JEL classification: G11, G13

Keywords: Cryptocurrencies, risk management, hedging, copulas

*Department of Business and Economics, Berlin School of Economics and Law, Badensche Str. 52, 10825 Berlin, Germany. Blockchain Research Center, Humboldt-Universität zu Berlin, Germany. International Research Training Group 1792, Humboldt-Universität zu Berlin, Germany. E-mail: Francis.Liu@hwr-berlin.de.

†Department of Business and Economics, Berlin School of Economics and Law, Badensche Str. 52, 10825 Berlin, Germany. International Research Training Group 1792, Humboldt-Universität zu Berlin, Germany. E-mail: packham@hwr-berlin.de.

‡Department of Finance, Asia University, 500, Lioufeng Rd., Wufeng, Taichung 41354, Taiwan Department of Finance, Asia University, 500, Lioufeng Rd., Wufeng, Taichung 41354, Taiwan E-mail: mangrou@gmail.com.

§Blockchain Research Center, Humboldt-Universität zu Berlin, Germany. Wang Yanan Institute for Studies in Economics, Xiamen University, China. Sim Kee Boon Institute for Financial Economics, Singapore Management University, Singapore. Faculty of Mathematics and Physics, Charles University, Czech Republic. National Yang Ming Chiao Tung University, Taiwan. E-mail: haerdle@wiwi.hu-berlin.de.

¶Financial support of the European Union's Horizon 2020 research and innovation program "FIN-TECH: A Financial supervision and Technology compliance training programme" under the grant agreement No 825215 (Topic: ICT-35-2018, Type of action: CSA), the European Cooperation in Science & Technology COST Action grant CA19130 - Fintech and Artificial Intelligence in Finance - Towards a transparent financial industry, the Deutsche Forschungsgemeinschaft's IRTG 1792 grant, the Yushan Scholar Program of Taiwan the Czech Science Foundation's grant no. 19-28231X / CAS: XDA 23020303, as well as support by Ansar Aynetdinov (ansar.aynetdinov@hu-berlin.de) are greatly acknowledged.

Contents

1 Introduction

Cryptocurrencies (CC's) are a fast-growing asset class, with many more CCs now available on the market since the first cryptocurrency Bitcoin (BTC) surfaced (Nakamoto, 2009). In response to the rapid development of the CC market, the CME Group launched exchange-traded BTC futures contracts in December 2017. At the time of writing, the CME is the only exchanged offering regulated crypto futures. The average daily volume and open interest of the CME BTC futures are $2,518 M and $2,836 M respectively.*[Add an approximate date. Where are these figures from?]* Because it is regulated, the CME BTC derivatives market is an attractive way for institutional investors to participate in or manage their exposure in the crypto market. As more individual and institutional investors are adding CCs and CC derivatives to their portfolios, the need to understand downside risks and find suitable ways to hedge against extreme risks is created. Fom a risk management perspective, the roller-coaster ride of crypto prices may create significant basis risk, even when using simple hedges involving crypto portfolios and BTC futures. This requires analysing the dependence structure of cryptos and futures beyond linear correlation.

In this paper, we examine static hedges of crypto portfolios with Bitcoin futures. Owing to the asymmetry of crypto returns as well as the occurrence of extreme events, we consider different dependence structures via a variety of copula models. We then optimise the hedge ratio using different risk measures. A similar study was conducted by (Barbi and Romagnoli, 2014) for equity and FX portfolios. Barbi and Romagnoli (2014)'s work is based on Cherubini et al. (2011) to derive the distribution of linear combinations of margins with copulae describing the dependence structure. We slightly extend their results and come up with a formula for the linear combination of random variables for our purpose.

The hedge ratio is the appropriate amount of futures contracts to hold in order to eliminate the risk exposure in the underlying security. The determination of the optimal hedge ratio relies primarily on the dependence between BTC and futures prices. Financial asset returns have long known to be non-Gaussian, see e.g. (Fama, 1963; Cont, 2001). Specifically, Gaussian models cannot produce the heavy tails and the asymmetry observed in asset returns, which in turn implies a consistent underestimation of financial risks. Therefore, to minimize downside risk, one cannot solely rely on second-order moment calculations. Moreover, variance as a risk measure does not account for the variety of investors' utility functions. In particular, it is known that investors are tail-risk averse, see Menezes et al. (1980). Copulae provide the flexibility to model multivariate random variables separately by their margins and dependence structure. The concept of copulae was originally developed (but not under this name) by Wassily Hoeffding (Hoeffding, 1940a) and later popularised by the work of Abe Sklar (Sklar, 1959).

Different risk measures account for investors' risk attitudes. They serve as loss functions in the search process of the optimal hedge ratio. Of the vast literature discussing the relationship between risk measures and investors' risk attitudes, we refer readers to Artzner et al. (1999) for an axiomatic approach of risk measure construction; Embrechts et al. (2002) for reasoning of using expected shortfall (ES) and spectral risk measures (SRM) in addition to value-at-risk (VaR); Acerbi (2002) for direct linkages between risk measures and investor's risk attitudes using the concept of a "risk aversion function".

In order to capture a variety of risk preferences, in addition to variance, we include the risk measures value-at-risk (VaR), expected shortfall (ES), and spectral risk measures (SRM). VaR is widely used by the finance industry and easy to understand. ES and SRM are chosen because of their coherence property, in particular, they recognize diversification benefits. SRM can also be directly related to an individual's utility function. Examples are the exponential SRM and power SRM introduced by Dowd et al. (2008).

In this work, we study the effectiveness of hedging various CC's and crypto indices using Bitcoin futures under copula models and different risk preferences. In an extensive back-test,[1] we find the ability of the BTC futures to hedge BTC and BTC-related indices promising, regardless of the choices of the copula (with the exception of the Frank copula) and risk measure. On the other hand, the ability of BTC futures to hedge other cryptos depends on various factors, such as ... (was: is inconclusive) *[Something more useful should be said here. "is inconclusive" means: "stop reading here"]*. Instead of suggesting a particular copula or risk measures, we discuss the characteristics of different settings.

The paper is organized as follows. Section 2 introduces the notion of an optimal hedge ratio; Section 3 decribes the method of estimation of copulae; Section 4 provides the empirical result; Section 5 concludes. All calculations in this work can be reproduced with the data and code available at www.quantlet.com .

2 Optimal hedge ratio

2.1 Distribution of hedge portfolio

We form a portfolio with two assets, consisting of one unit in the spot asset and a short position of h units of a futures contract, for example one Bitcoin and a short position in a CME Bitcoin futures contract. The objective is to minimize the risk of the exposure in the spot. Let R^S and R^F be the (discrete) returns of the spot and futures price. The (discrete) return of the portfolio is[2]

$$R^h = R^S - hR^F.$$

[I fixed this, please check.] [We need to discuss the footnote. Generally, the portfolio return is $R_p = \sum_{i=1}^n w_i R_i$. With the futures contract, the notional investment in the futures is zero, so the portfolio return is $(S_0(1+R^S) - hF_0R^F)/S_0 - 1 = R^S - hR^F$, if $S_0 = F_0$.]

To measure risk, we define a risk measure ρ to be a mapping from a financial position or its return, such as R^h, to a real number, which is often interpreted as the amount of money to make the position acceptable (e.g. to a regulator), see e.g. (Föllmer and Schied, 2002). For example, a widely used risk measure is value-at-risk (VaR), which, at the confidence level α, is derived from the $1-\alpha$ quantile of the return distribution.

If the portfolio reduces the risk of the spot position, then we call this a hedge portfolio. An optimal hedge ratio h^* is a parameter that minimizes the risk of the aforementioned portfolio

$$h^* = \operatorname*{argmin}_h \rho(R^h).$$

Obviously the cdf and pdf of R^h and the risk measure depend on the joint distribution of R^S and $-hR^F$. However, optimising h according to $f_{R^S,-hR^F}$ is unfavorable since one would need to calibrate the joint pdf $f_{R^S,-hR^F}$ whenever updating h. Another problem of using the joint pdf is that one lacks the flexibility to model the margins separately from the dependence structure. Copulae allow to

[1] We thank the data provider Tiingo (https://www.tiingo.com/) for providing the crypto price data.

[2] In practice, as the nominal investment in the futures is zero, R^F is understood as the return on the notional amount underlying the futures contract. In other words, if both the spot price S_{t-1} and the futures price F_{t-1} are normalised to 1, then the portfolio return will be identical to the portfolio value change $\Delta V = \Delta S - h\Delta F$, where $\Delta S = S_t - S_{t-1}$, etc.

overcome both of these problems.

The advantage of using copulae is two-fold. First, copulae are invariant under strictly monotone increasing function (Schweizer et al., 1981), a property used in Lemma 1 below. Second, copulae allow us to model the margins and dependence structure separately, a result known as Sklar's Theorem (Sklar, 1959), which is given as Theorem 1 below. See also (Nelsen, 1999; Joe, 1997; McNeil et al., 2005) for Sklar's Theorem and more properties of copulae.

[I find it tricky that we give Sklar's Theorem, but no definition of a copula. This should be added.]

Theorem 1 (Hoeffding-Sklar-Theorem) *Let F be a joint distribution function with marginal distributions F_X and F_Y. Then, there exists a copula $C : [0,1]^2 \mapsto [0,1]$ such that, for all $x, y \in \mathbb{R}$*

$$F(x,y) = C\{F_X(x), F_Y(y)\}. \tag{1}$$

If the margins are continuous, then C is unique; otherwise C is unique on the range of the margins.

Conversely, if C is a copula and F_X, F_Y are univariate distribution functions, then the function F defined by (1) is a joint distribution function with margins F_X, F_Y.

Indeed, many basic results about copulae can be traced back to early works of Wassily Hoeffding (Hoeffding, 1940b, 1941). The works aimed to derive a measure of relationship of variables, which is invariant under change of scale. See also Fisher and Sen (2012) for English translations of the original papers written in German.

Lemma 1 *Let $h > 0$ and let X and Y be continuous random variables. Then, the joint distribution of the portfolio positions can be expressed via the joint distribution of the securities as follows:*

$$C_{X,hY}\left(F_X(s), F_{hY}(t)\right) = C_{X,Y}\left(F_X(s), F_Y(t/h)\right), \quad s,t \in \mathbb{R}. \tag{2}$$

Proof. Since copulae are invariant under strictly monotone increasing function (Schweizer et al., 1981, Theorem 3 (i)) or (Nelsen, 1999, Theorem 2.4.3),

$$C_{X,hY}\left(F_X(s), F_{hY}(t)\right) = C_{X,Y}\left(F_X(s), F_{hY}(t)\right).$$

Re-writing the second argument of the copula gives

$$F_{hY}(t) = \mathbb{P}(hY \le t) = \mathbb{P}(Y \le t/h) = F_Y(t/h).$$

∎

Leveraging these two features of copulae, Barbi and Romagnoli (2014) introduce the distribution of linear combinations of random variables using copulae. We slightly edit their Corollary 2.1 of their work and yield the following expression of the distribution.

Proposition 2 *Let X and Y be two real-valued continuous random variables on a probability space $(\Omega, \mathcal{F}, \mathbf{P})$ with absolutely continuous copula $C_{X,Y}$ and marginal distribution functions F_X and F_Y. Then, the distribution function of Z* [What is Z?] *is given by*

$$F_Z(z) = 1 - \int_0^1 D_1 C_{X,Y}\left[u, F_Y\left\{\frac{F_X^{(-1)}(u) - z}{h}\right\}\right] du, \tag{3}$$

where, $F^{(-1)}$ denotes the inverse of F, i.e., the quantile function. [Please check, but this holds only for $h > 0$.]

Here, $D_1C(u, v) = \dfrac{\partial}{\partial u}C(u, v)$ and, see e.g. Equation (5.15) of (McNeil et al., 2005),

$$D_1C_{X,Y}\{F_X(x), F_Y(y)\} = \mathbf{P}(Y \leq y|X = x). \tag{4}$$

Proof. Using the identity (4) gives

$$\begin{aligned} F_Z(z) &= \mathbf{P}(X - hY \leq z) = \mathbb{E}\left\{\mathbf{P}\left(Y \geq \frac{X-z}{h}\Big|X\right)\right\} \\ &= 1 - \mathbb{E}\left\{\mathbf{P}\left(Y \leq \frac{X-z}{h}\Big|X\right)\right\} = 1 - \int_0^1 D_1C_{X,Y}\left[u, F_Y\left\{\frac{F_X^{(-1)}(u) - z}{h}\right\}\right] du. \end{aligned}$$

■

Corollary 1 *Given the formulation of random variables* [What exactly does this mean?]*, the pdf of Z can be written as* [Since $h > 0$, it is sufficient to write $1/h$. Order of arguments in $c_{X,Y}$ must be flipped.]

$$f_Z(z) = \left|\frac{1}{h}\right| \int_0^1 c_{X,Y}\left[F_Y\left\{\frac{F_X^{(-1)}(u) - z}{h}\right\}, u\right] \cdot f_Y\left\{\frac{F_X^{(-1)}(u) - z}{h}\right\} du, \tag{5}$$

or

$$f_Z(z) = \int_0^1 c_{X,Y}\left[F_X\left\{z + hF_Y^{(-1)}(u)\right\}, u\right] \cdot f_X\left\{z + hF_Y^{(-1)}(u)\right\} du. \tag{6}$$

The two expressions are equivalent. *[This is obvious as their LHS's agree... I think you want to say something else. How is the second expression obtained?]* Note that the pdf of Z in the above proposition can be assessed via numerical integration as long as we have the copula density and the marginal densities. A generic expression *[Of what?]* and proof can be found in the appendix. *[Reference appendix properly.]*

2.2 Procedure to determine optimal hedge ratio

We introduce the empirical procedure to obtain the optimal hedge ratio being used in this work. *[This is really the backtesting procedure. I think it'd be good if the word "backtest" appeared somwewhere.]* First, we split the time series of spot and futures into sets of training and testing data. *[test data?]* The training data makes up the first 300 observations and its corresponding testing data consists of the consecutive 5 observations. We then roll 5 observations forward (step size of 5) to obtain the next training and test data sets and repeat this until the end of the time series. Note that the testing data are non-overlapping since the step size is equal to test size.

Next, we obtain the optimal hedge ratio as follows:

1. **Construct univariate kernel density function (KDE)**. From the training data we calibrate the spot and futures' univariate kernel density functions using the Gaussian kernel with bandwidth determined by the refined plug-in method (Härdle et al., 2004, section 3.3.3).

2. **Calibrate copulae**. We then calibrate the copulae outlined in section 3.1 via the method of moments described in section 3.2.1.

3. **Select copula**. We compute the Akaike Information Criterion. The copula with the best (i.e., lowest) AIC is used for the next step. A discussion of this step is found in 3.2.3.

4. **Determine optimal hedge ratio**. We determine the optimal hedge ratios numerically using different risk measures as the loss function by drawing samples from the selected copula and KDEs. The risk measures used as risk reduction objectives are outlined in 3.3

5. **Obtain log-return of hedged portfolio on test data set**. Finally, we apply the optimal hedge ratios to the test data $R_h = R_s - h^* R_f$.

3 Copulae and risk measures

3.1 Copulae

To capture different aspects of the dependence structure, we consider a set of different copulas, which are layed out in detail below. These are the Gaussian-, t-, Frank-, Gumbel-, Clayton-, mixture, NIG factor, and Plackett-copula.

As this hedging backtest concerns only portfolios with two assets, we focus on the bivariate version of each copula and bivariate copula measures, such as Kendall's τ_K and Spearman's ρ_S.

3.1.1 Copula measures

Kendall's τ and Spearman's ρ are measures of association in terms of concordance, see Kruskal (1958). *[A number of definitions follow. It usually helps the reader if they are put in a definition block rather than just flowing with the text.]* Let (x_i, y_i) and (x_j, y_j) denote two realisations of a vector (X, Y) of continuous random variables. A pair of observations is concordant if $x_i < x_j$ and $y_i < y_j$, discordant if $x_i > x_j$ and $y_i < y_j$ or if $x_i < x_j$ and $y_i > y_j$. *[What about the case $x_i > x_j$ and $y_i > y_j$?]* For a bivariate random variable of n observations, there are $\binom{n}{2}$ distinct pairs. *[I struggled with understanding what "distinct pairs" refers to, but found the answer in Nelsen. Perhaps add a little more test. Also, as this paragraph seems to be taken directly from Nelsen, it* **must** *be cited accordingly!]*

Let c denote the number of concordant pairs, and d the number of discordant pairs. Kendall's tau is defined as follows: (Nelsen, 1999)

$$\tau_K := \frac{c-d}{c+d} = \frac{c-d}{\binom{n}{2}}.$$

Let F_X and F_Y be the cdfs of X and Y respectively, Spearman's ρ is *[These are two sentences, so please separate them into two sentences. Also, formulas belong syntactically to the sentence, so if they end the sentence, there should be a full stop.]*

$$\rho_S := 12\mathbb{E}(F_X(X)F_Y(Y)) - 3.$$

[Is there a particular reason to switch between sample and population versions?]

Upper tail dependence is defined as *[Typeset terms that are defined, e.g. upper tail dependence, in italics.]*

$$\lambda_U := \lim_{q \to 1^-} \mathbf{P}\{X > F_X^{(-1)}(q) | Y > F_Y^{(-1)}(q)\};$$

Lower tail dependence is defined as

$$\lambda_L := \lim_{q \to 0^+} \mathbf{P}\{X \leq F_X^{(-1)}(q) | Y \leq F_Y^{(-1)}(q)\}.$$

Furthermore, we denote the Fréchet-Hoeffding lower bound by $\boldsymbol{W}$, the product copula by $\boldsymbol{\Pi}$, and the Fréchet-Hoeffding upper bound by $\boldsymbol{M}$. They represent cases of perfect negative dependence, independence, and perfect positive dependence, respectively. For further details, we refer readers to Joe (1997) and Nelsen (1999); see also Härdle and Okhrin (2010).

The symmetry property of copulae is also important for modelling financial data. In particular, we are interested in radial symmetry among various concepts of symmetry, see Nelsen (1999). *[Why?]*

Definition 3 *Let $(U_1, ..., U_d)$ be random variables.* [uniform on $[0,1]$?] *The random variables is radially symmetric if the joint cdf of $(U_1, ..., U_d)$ is same as the joint cdf of $(1 - U_1, ..., 1 - U_d)$*

3.1.2 Gaussian and t Copulae

The Gaussian and t copulae are dervived from Gaussian and t distributions. As the Gaussian and t distributions belong to the family of elliptical distributions, their copulae belong to the family of elliptical copulae. *[I personally would remove the reference to the elliptical family, as this is not important for what is to come. If it must stay, then briefly explain what elliptical distributions are ("Empirical distributions are characterised by...".]*

The bivariate Gaussian copula is defined as

$$\begin{aligned} \boldsymbol{C}(u, v) &= \Phi_{2,\rho}\{\Phi^{(-1)}(u), \Phi^{(-1)}(v)\} \\ &= \int_{-\infty}^{\Phi^{(-1)}(u)} \int_{-\infty}^{\Phi^{(-1)}(v)} \frac{1}{2\pi\sqrt{1-\rho^2}} \exp\left\{\frac{s^2 - 2\rho st + t^2}{2(1-\rho^2)}\right\} \mathrm{d}s \, \mathrm{d}t, \quad , u, v \in [0, 1], \end{aligned}$$

where $\Phi_{2,\rho}$ is the bivariate Normal cdf with zero mean, unit variance, and correlation coefficient ρ, and $\Phi^{(-1)}$ is the quantile function of the univariate standard normal distribution. The Gaussian copula is fully specified by the correlation parameter ρ. [3] Like all elliptical copulas, it is symmetric. *[Remove reference to elliptic copula.]* It has no tail dependence, which, in a finance context, implies that it often underestimates tail risk.

The Gaussian copula density is

$$\boldsymbol{c}_\rho(u, v) = \frac{\boldsymbol{\varphi}_{2,\rho}\{\Phi^{(-1)}(u), \Phi^{(-1)}(v)\}}{\varphi\{\Phi^{(-1)}(u)\} \cdot \varphi\{\Phi^{(-1)}(v)\}} = \frac{1}{2\pi\sqrt{1-\rho^2}} \exp\left\{-\frac{u^2 - 2\rho uv + v^2}{2(1-\rho^2)}\right\},$$

where $\boldsymbol{\varphi}_{2,\rho}(\cdot)$ is the pdf corresponding to $\Phi_{2,\rho}$, and $\varphi(\cdot)$ the standard normal pdf. *[I think the abbreviations cdf and pdf where not introduced. Please double-check.]*

To illustrate the various copulae and their differences, Figure 1 shows scatter plots of random samples of each of the copulae treated.

[3] The symbol ρ is used to denote both the correlation parameter as well as a general risk measure. However, it will be clear from the context, what ρ refers to.

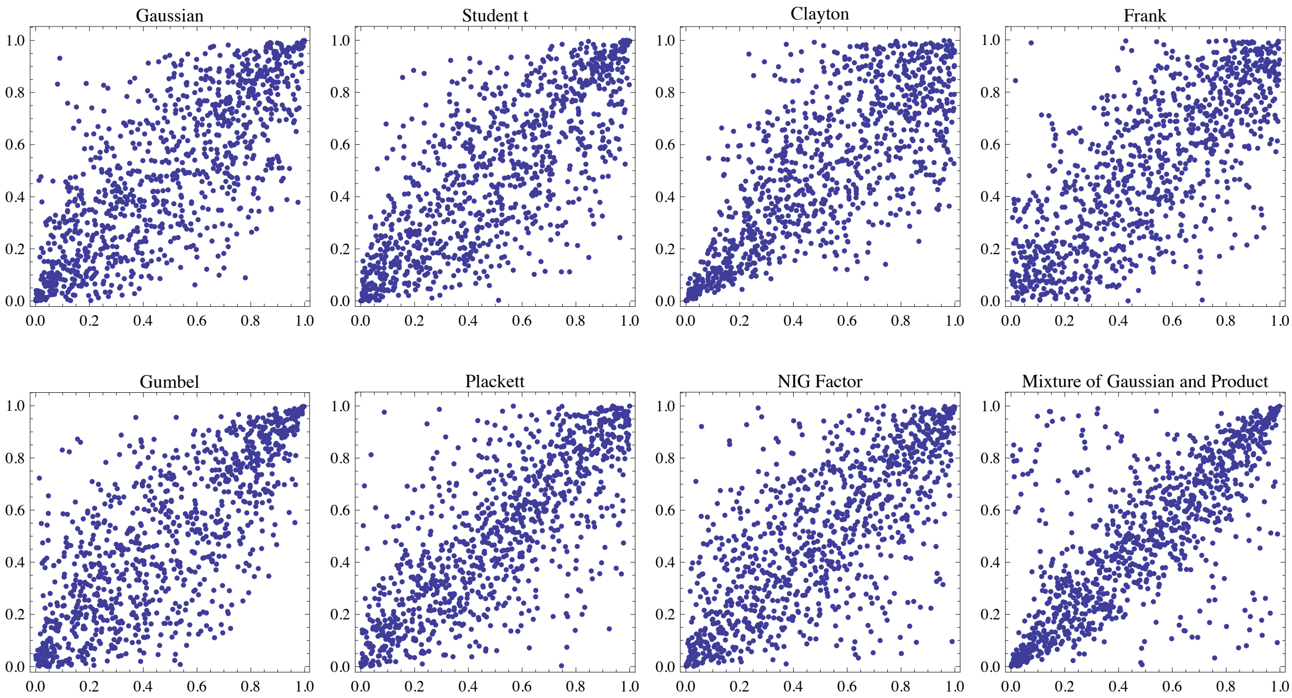

Figure 1: Scatterplots of samples drawn from various copulae. All copulae are calibrated to Spearman's ρ of 0.75 before sampling.

Kendall's τ_K and Spearman's ρ_S of the bivariate Gaussian copula are

$$\tau_K(\rho) = \frac{2}{\pi} \arcsin \rho$$

$$\rho_S(\rho) = \frac{6}{\pi} \arcsin \frac{\rho}{2}.$$

The t-copula has the form

$$\begin{aligned} \boldsymbol{C}(u,v) &= \boldsymbol{T}_{2,\rho,\nu}\{T_\nu^{(-1)}(u), T_\nu^{(-1)}(v)\} \\ &= \int_{-\infty}^{T_\nu^{(-1)}(u)} \int_{-\infty}^{T_\nu^{(-1)}(v)} \frac{\Gamma\left(\frac{\nu+2}{2}\right)}{\Gamma\left(\frac{\nu}{2}\right)\pi\nu\sqrt{1-\rho^2}} \left(1 + \frac{s^2 - 2st\rho + t^2}{\nu}\right)^{-\frac{\nu+2}{2}} \mathrm{d}s\,\mathrm{d}t, \end{aligned}$$

where $\boldsymbol{T}_{2,\rho,\nu}$ denotes the bivariate t cdf with dependence parameter ρ *[Is this Spearman's Rho? If so, then say so.]* and degrees of freedom parameter ν, $\nu > 2$, and where $T_\nu^{(-1)}(\cdot)$ is the quantile function of a standard t distribution with parameter ν.

Contrary to the Gaussian copula, the t-copula has a non-zero tail dependence coefficient, which makes it more appropriate for dependence modelling in finance. The Gaussian copula arises as $\nu \to \infty$.

The copula density is

$$\boldsymbol{c}(u,v) = \frac{\boldsymbol{t}_{2,\rho,\nu}\{T_\nu^{(-1)}(u), T_\nu^{(-1)}(v)\}}{t_\nu\{T_\nu^{(-1)}(u)\} \cdot t_\nu\{T_\nu^{(-1)}(v)\}},$$

where $\boldsymbol{t}_{2,\rho,\nu}$ is the pdf of $\boldsymbol{T}_{2,\rho,\nu}$ and t_ν the density of standard t distribution.

The t-copula and Gaussian copula with parameter ρ have equal Kendall's τ, a property shared by all so-called elliptical copulas (see Demarta and McNeil, 2005, and references therein). (was: Like all the other elliptical copulae, the t-copula's Kendall's τ is identical to that of the Gaussian copula (see Demarta and McNeil, 2005, and references therein).)

3.1.3 Archimedean copulae

The family of Archimedean copulae forms a large class of copulae with many convenient features. Archimedean copulas are determined via a simple parametric form of the dependence structure. A prominent feature is the ability to model asymmetric dependence structures.

In general, an Archimedean copula takes the form

$$\boldsymbol{C}(u,v) = \psi^{(-1)}\{\psi(u), \psi(v)\}, \quad u, v \in [0,1],$$

where $\psi : [0,1] \to [0,\infty)$ is a continuous, strictly decreasing and convex function such that $\psi(1) = 0$ *[Where does θ come in?]* for any permissible dependence parameter θ. The function ψ is called the generator, with $\psi^{(-1)}$ its inverse.

The *Frank copula* (B3 in Joe (1997)) takes the form

$$\boldsymbol{C}_\theta(u,v) = \frac{1}{\theta}\log\left\{1 + \frac{(e^{-\theta u}-1)(e^{-\theta v}-1)}{e^{-\theta}-1}\right\}, \quad u, v \in [0,1],$$

with $\theta \in [0,\infty]$ the dependence parameter. It is a radially symmetric copula and cannot produce any tail dependence. The following parameters correspond perfect dependence and independence: $\boldsymbol{C}_{-\infty} = \boldsymbol{M}$, $\boldsymbol{C}_1 = \boldsymbol{\Pi}$, and $\boldsymbol{C}_\infty = \boldsymbol{W}$. The copula density is

$$\boldsymbol{c}_\theta(u,v) = \frac{\theta e^{\theta(u+v)(e^\theta - 1)}}{\left\{e^\theta - e^{\theta u} - e^{\theta v} + e^{\theta(u+v)}\right\}^2}.$$

The Frank copula has Kendall's τ and Spearman's ρ as follow:

$$\tau_K(\theta) = 1 - 4\frac{D_1\{-\log(\theta)\}}{\log(\theta)},$$

and

$$\rho_S(\theta) = 1 - 12\frac{D_2\{-\log(\theta)\} - D_1\{\log(\theta)\}}{\log(\theta)},$$

where D_1 and D_2 are the Debye function of order 1 and 2, with the Debye function defined as $D_n = \frac{n}{x^n}\int_0^x \frac{t^n}{e^t - 1}dt$. *[Please find a reference for the Debye function. A good candiate is the Handbook by Abramowitz Stegun.]*

The *Gumbel copula* (B6 in Joe (1997)) has distribution function

$$\boldsymbol{C}_\theta(u,v) = \exp - \{(-\log(u))^\theta + (-\log(v))^\theta\}^{\frac{1}{\theta}},$$

where $\theta \in [1,\infty)$ is the dependence parameter. It has upper tail dependence with dependence parameter $\lambda^U = 2 - 2^{\frac{1}{\theta}}$ and displays no lower tail dependence.

While the Gumbel copula cannot model perfect counter-dependence (Nelsen, 2002), $\boldsymbol{C}_1 = \boldsymbol{\Pi}$ models independence, and $\lim_{\theta\to\infty} \boldsymbol{C}_\theta = \boldsymbol{W}$ models perfect dependence. The copula density takes the form

$$\tau_K(\theta) = \frac{\theta - 1}{\theta}.$$

The *Clayton copula* takes the form

$$\boldsymbol{C}_\theta(u,v) = \left\{\max(u^{-\theta} + v^{-\theta} - 1, 0)\right\}^{-\frac{1}{\theta}},$$

where $\theta \in (-\infty, \infty)$ is the dependence parameter. The Clayton copula, by contrast to Gumbel copula, generates lower tail dependence with $\lambda^L = 2^{-\frac{1}{\theta}}$, but cannot generate upper tail dependence. Moreover, $\lim_{\theta\to-\infty} \boldsymbol{C}_\theta = \boldsymbol{M}$, $\boldsymbol{C}_0 = \boldsymbol{\Pi}$, and $\lim_{\theta\to\infty} \boldsymbol{C}_\theta = \boldsymbol{W}$. Kendall's τ of the Clayton copula is given by

$$\tau_K(\theta) = \frac{\theta}{\theta + 2}.$$

3.1.4 Mixture Copula

The mixture copula is a linear combination of copulae. The distribution of a 2-dimensional random variable $\boldsymbol{X} = (X_1, X_2)^\top$ is written as linear combination of K copulae

$$\boldsymbol{C}(u,v) = \sum_{k=1}^{K} p^{(k)} \cdot \boldsymbol{C}^{(k)}\{F_{X_1}^{(-1)}(u), F_{X_2}^{(-1)}(v); \boldsymbol{\theta^{(k)}}\}, \quad u, v \in [0,1].$$

Here, $\boldsymbol{\theta^{(k)}}$ refers to the parameters of the k-th copula. Likewise, the copula density is a linear combination of copula densities

$$\boldsymbol{c}(u,v) = \sum_{k=1}^{K} p^{(k)} \cdot \boldsymbol{c}^{(k)}\{F_{X_1}^{(-1)}(u), F_{X_2}^{(-1)}(v); \boldsymbol{\theta^{(k)}}\}.$$

[I think the statement below can go without a formal proof. Here is a suggestion].

While Kendall's τ of the mixture copula is not known in closed form, Spearman's ρ is easily derived as

$$\rho_S = \sum_{k=1}^{K} p^{(k)} \cdot \rho_S^{(k)}.$$

[Old text below.]

While Kendall's τ of the mixture copula is not known in closed form, Spearman's ρ is specified by the following statement.

Proposition 4 *Let $\rho_S^{(k)}$ be Spearman's ρ of the k-th component Spearman's ρ of the mixture copula is given by*

$$\rho_S = \sum_{k=1}^{K} p^{(k)} \cdot \rho_S^{(k)}.$$

Proof. Since Spearman's ρ is defined as (Nelsen, 1999)

$$\rho_S = 12 \int_{\mathbb{I}^2} \boldsymbol{C}(s,t) ds dt - 3,$$

Spearman's ρ of the the mixture copula is given by summation of the components

$$\rho_S = 12 \int_{\mathbb{I}^2} \sum_{k=1}^{K} p^{(k)} \cdot \boldsymbol{C}^{(k)}(s,t) ds dt - 3.$$

■ *[Continue here.]*

An example of a mixture copula is the Fréchet class of copulae, which are given by convex combinations of $\boldsymbol{W}$, $\boldsymbol{\Pi}$, and $\boldsymbol{M}$ (Nelsen, 1999).

We use a mixture of Gaussian and independence copulae in our analysis, i.e.,

$$\boldsymbol{C}(u,v) = p\,\boldsymbol{C}^{\text{Gaussian}}(u,v) + (1-p)(uv), \quad p \in (0,1),$$

with corresponding density

$$\boldsymbol{c}(u,v) = p\,\boldsymbol{c}^{\text{Gaussian}}(u,v) + (1-p).$$

This mixture models the amount of "random noise" that appears in the dependence structure. In the hedging exercise, the "random noise" adds an unhedgable component to the two-asset portfolio, whose weight $(1-p)$ is calibrated from market data. *[Is it clear that the unhedgable part is more than the "random noise"?]*

3.1.5 NIG factor copula

The *normal inverse Gaussian (NIG)* distribution, introduced by (Barndorff-Nielsen, 1997), has density function

$$g(x;\alpha,\beta,\mu,\delta) = \frac{\alpha}{\pi}\mathbf{e}^{\delta\sqrt{\alpha^2-\beta^2}-\beta\mu}\frac{1}{q((x-\mu)/\delta)}K_1\left[\delta\alpha q\left(\frac{x-\mu}{\delta}\right)\right]\mathbf{e}^{\beta x}, \quad x>0,$$

where $q(x) = \sqrt{1+x^2}$ and where K_1 is the modified Bessel function of third order and index 1. The parameters satisfy $0 \le |\beta| \le \alpha$, $\mu \in \mathbb{R}$ and $\delta > 0$. The parameters have the following interpretation: μ and δ are location and scale parameters, respectively, α determines the heaviness of the tails and β determines the degree of asymmetry. If $\beta = 0$, then the distribution is symmetric around μ.

The moment-generating function of the NIG distribution is given by

$$M(u;\alpha,\beta,\mu,\delta) = \exp\left(\delta\left(\sqrt{\alpha^2-\beta^2} - \sqrt{\alpha^2-(\beta+u)^2}\right) + \mu u\right).$$

As a direct consequence, moments are easily calculated with the expectation and variance of the NIG distribution being

$$\mathbb{E}X = \mu + \frac{\delta\beta}{\sqrt{\alpha^2-\beta^2}}$$

$$\operatorname{Var}(X) = \frac{\alpha^2\delta}{(\alpha^2-\beta^2)^{3/2}}. \tag{7}$$

The $\text{NIG}(\alpha,\beta,\mu\,\delta)$ distribution belongs to the class of so-called *normal variance-mean mixture distributions*, (see Section 3.2 of (McNeil et al., 2005)): X follows an $\text{NIG}(\alpha,\beta,\mu,\delta)$ distribution if X conditional on W follows a normal distribution with mean $\mu+\beta W$ and variance W, i.e.,

$$X|W \overset{\mathcal{L}}{\sim} \text{N}(\mu+\beta W, W),$$

where W follows an *inverse Gaussian distribution*, denoted by $\text{IG}(\delta, \sqrt{\alpha^2-\beta^2})$.

It is easily seen from the moment-generating function that the NIG distribution is preserved under linear combinations, provided the variables share the parameters α and β. For this and other reasons, the NIG distribution is popular in many areas of financial modelling; for example, it gives rise to the normal inverse Gaussian Lévy process, which may be represented as a Brownian motion with a time change.

In the setting here, we consider the *NIG factor copula*. This is not directly derived from the multivariate NIG distribution, but determined through a factor structure instead. The factor structure, which was applied e.g. in (Kalemanova et al., 2007) for calibrating CDO's, gives additionaly flexibility as it does not force the components to have a mixing variable W. The following proposition introduces the NIG factor model and some of its properties.

Proposition 5 *Let $Z \sim NIG(\alpha, \beta, \mu, \delta)$ and $Z_i \sim NIG(\alpha, \beta, \mu_i, \delta_i)$, $i = 1, \dots, n$ be independent NIG-distributed random variables. Then:*

1. $X_i = Z + Z_i \sim NIG(\alpha, \beta, \mu + \mu_i, \delta + \delta_i)$,
2. *and*

$$\begin{aligned} Cov(X_i, X_j) &= Var(Z), \\ Corr(X_i, X_j) &= \frac{\delta}{\sqrt{(\delta + \delta_i)(\delta + \delta_j)}}. \end{aligned} \tag{8}$$

Proof.

1. This follows directly from the moment-generating function.
2. For the covariance,

$$\mathrm{Cov}(X_i, X_j) = \mathbb{E}[(Z + Z_i)(Z + Z_j)] - \mathbb{E}[Z + Z_i]\mathbb{E}[Z + Z_j] = \mathbb{E}[Z^2] - (\mathbb{E}Z)^2.$$

The correlation is determined directly from 7.

■

[Please clarify that $\circ$ refers to composition. Clean up notation, e.g. marginals can be denoted F_F and F_S, Use just C for the copula. What are Z_1 and Z_2? I don't find the formula in the paper mentioned. Also, where is the formula for Kendall's tau taken from?] The NIG factor copula is obtained by transforming the margins to uniforms (see Sklar's Theorem), giving (e.g. (Krupskii and Joe, 2013)):

$$C_{r^S, r^F}(F_{r^S}(r^S), F_{r^F}(r^F)) = \int_{\mathbb{R}} F_{Z_1}(F_{X_1}^{(-1)} \circ F_{r^S}(r^S) - z) \cdot F_{Z_2}(F_{X_2}^{(-1)} \circ F_{r^F}(r^F) - z) \cdot f_Z(z) dz.$$

If the margins are continuous, then Spearman's rho of NIG factor copula is

$$\rho_S = 12 \int\int\int_{\mathbb{R}^3} F_{X_1}(x_1) \cdot F_{X_2}(x_2) \cdot f_{Z_1}(x_1 - z) \cdot f_{Z_2}(x_2 - z) \cdot f_Z(z) dx_1 dx_2 dz - \frac{1}{48}.$$

3.1.6 Plackett copula

The Plackett copula has distribution functiono

$$\boldsymbol{C}_\theta(u, v) = \frac{1 + (\theta - 1)(u + v)}{2(\theta - 1)} - \frac{\sqrt{\{1 + (\theta - 1)(u + v)\}^2 - 4uv\theta(\theta - 1)}}{2(\theta - 1)},$$

where θ.... Spearman's Rho is given by

$$\rho_S(\theta) = \frac{\theta+1}{\theta-1} - \frac{2\theta\log\theta}{(\theta-1)^2}.$$

The Placket copula possesses a special property, namely the cross-product ratio is equal to the dependence parameter

$$\frac{\mathbf{P}(U \le u, V \le v) \cdot \mathbf{P}(U > u, V > v)}{\mathbf{P}(U \le u, V > v) \cdot \mathbf{P}(U > u, V \le v)} = \frac{\boldsymbol{C}_\theta(u,v)\{1-u-v+\boldsymbol{C}_\theta(u,v)\}}{\{u-\boldsymbol{C}_\theta(u,v)\}\{v-\boldsymbol{C}_\theta(u,v)} = \theta.$$

In words, the dependence parameter is equal to the ratio of the number of concordance pairs and the number of discordance pairs of a bivariate random variable.

3.2 Calibration and selection of copulae

We introduce the method to calibrate copulae to our data in this section. In general, there are two types of calibration procedures to calibrate copulae: maximum likelihood (MLE) and method of moments (MM). We decide to deploy the latter since it calibrates according to the moments desired. *[This is a long way of saying very little; is it possible to shorten it?]*

In the following subsection, we present the configuration of the method of moments procedures in this work. In the Subsection 3.2.2, we demonstrate that MM is more suitable to this work by comparing MM with MLE.

3.2.1 Method of moments

We trace back the usage of MM to calibrate copulae to Genest (1987); Genest and Rivest (1993). The moments mainly refer to Kendall's τ or Spearman's ρ. We extend MM to quantile dependence measures denoted by λ_q for quantile level q. *[Please check, but I am fairly sure that we are not the first to extend MM to include quantiles! It must be clear that the method outlined here is not new or developed by us. Please cite (Oh and Patton, 2013) as well.]*

Spearman's ρ, Kendall's τ, and quantile dependence of the copula C are defined as

$$\begin{aligned}
\rho_S &= 12\int\int_{I^2} C_{\boldsymbol{\theta}}(u,v)\,\mathrm{d}u\,\mathrm{d}v - 3\\
\tau_K &= 4\mathbb{E}[C_{\boldsymbol{\theta}}\{F_X(x), F_Y(y)\}] - 1,\\
\lambda_q &= \begin{cases} \mathbf{P}(F_X(X) \le q | F_Y(Y) \le q) = \dfrac{C_{\boldsymbol{\theta}}(q,q)}{q}, & \text{if } q \in (0, 0.5],\\ \mathbf{P}(F_X(X) > q | F_Y(Y) > q) = \dfrac{1-2q+C_{\boldsymbol{\theta}}(q,q)}{1-q}, & \text{if } q \in (0.5, 1).\end{cases}
\end{aligned}$$

The empirical counterparts are

$$\hat{\rho}_S = \frac{12}{n}\sum_{k=1}^{n}\hat{F}_X(x_k)\hat{F}_Y(y_k) - 3,$$

$$\hat{\tau}_K = \frac{4}{n}\sum_{k=1}^{n}\hat{C}\{\hat{F}_X(x_i),\hat{F}_X(y_i)\} - 1,$$

$$\hat{\lambda}_q = \begin{cases} \dfrac{1}{n}\displaystyle\sum_{k=1}^{n}\frac{\mathbf{1}_{\{\hat{F}_X(x_k)\le q,\hat{F}_Y(y_k)\le q\}}}{q}, & \text{if } q\in(0,0.5],\\ \dfrac{1}{n}\displaystyle\sum_{k=1}^{n}\frac{\mathbf{1}_{\{\hat{F}_X(x_k)> q,\hat{F}_Y(y_k)> q\}}}{1-q}, & \text{if } q\in(0.5,1), \end{cases}$$

where $\hat{F}(x) = \frac{1}{n}\sum_{k=1}^{n} 1_{\{x_i\le x\}}$ and $\hat{C}(u,v) = \frac{1}{n}\sum_{k=1}^{n} 1_{\{u_i\le u, v_i\le v\}}$.

Denote by $\boldsymbol{m}(\boldsymbol{\theta})$ the m-dimensional vector of dependence measures according the dependence parameters $\boldsymbol{\theta}$,and let $\hat{\boldsymbol{m}}$ be the corresponding empirical counterpart. The difference between dependence measures and their counterpart is denoted by

$$\boldsymbol{g}(\boldsymbol{\theta}) = \hat{\boldsymbol{m}} - \boldsymbol{m}(\boldsymbol{\theta}),$$

and the MM estimator is

$$\hat{\boldsymbol{\theta}} = \underset{\boldsymbol{\theta}\in\boldsymbol{\Theta}}{\operatorname{argmin}}\, \boldsymbol{g}(\boldsymbol{\theta})^\top \hat{\boldsymbol{W}}\boldsymbol{g}(\boldsymbol{\theta}),$$

where $\hat{W}$ is a positive definite weight matrix. In this work, we use $\boldsymbol{m}(\boldsymbol{\theta}) = (\rho_S, \lambda_{0.05}, \lambda_{0.1}, \lambda_{0.9}, \lambda_{0.95})^\top$ for calibration with $\hat{W}$ set to the identity matrix. *[Is it right that we do not have Kendall's τ in our calibration? I suggest to add a sentence why.]*

3.2.2 Comparison between method of moments and maximum likelihood

By the Hoeffding-Sklar Theorem (Theorem 1), the joint density of a d-dimensional random variable $\boldsymbol{X}$ with sample size n can be written as

$$\boldsymbol{f_X}(x_1,...,x_d) = \boldsymbol{c}\{F_{X_1}(x_1),...,F_{X_d}(x_d)\}\prod_{j=1}^{d} f_{X_i}(x_i).$$

We follow the treatment of MLE documented in section 10.1 of Joe (1997), namely the *inference functions for margins (IFM) method*. The log-likelihood $\sum_{i=1}^{n}\boldsymbol{f_X}(X_{i,1},...,X_{i,d})$ can be decomposed into a dependence part and a marginal part,

$$\begin{aligned} L(\boldsymbol{\theta}) &= \sum_{i=1}^{n}\boldsymbol{c}\{F_{X_1}(x_{i,1};\boldsymbol{\delta}_1),...,F_{X_d}(x_{i,d};\boldsymbol{\delta}_d);\boldsymbol{\gamma}\} + \sum_{i=1}^{n}\sum_{j=1}^{d} f_{X_j}(x_{i,j};\boldsymbol{\delta}_j) \\ &= L_C(\boldsymbol{\delta}_1,...,\boldsymbol{\delta}_d,\boldsymbol{\gamma}) + \sum_{j=1}^{d} L_j(\boldsymbol{\delta}_j) \end{aligned}$$

where $\boldsymbol{\delta}_j$ are the parameters of the j-th margin, $\boldsymbol{\gamma}$ is the parameter of the parametric copula, and $\boldsymbol{\theta} = (\boldsymbol{\delta}_1,...,\boldsymbol{\delta}_d,\boldsymbol{\gamma})$. Instead of searching the $\boldsymbol{\theta}$ in a high dimensional space, Joe (1997) suggests to search for $\hat{\boldsymbol{\delta}}_1,...,\hat{\boldsymbol{\delta}}_d$ that maximize $L_1(\boldsymbol{\delta}_1),...,L_d(\boldsymbol{\delta}_d)$, then search for $\hat{\boldsymbol{\gamma}}$ that maximize $L_C(\hat{\boldsymbol{\delta}}_1,...,\hat{\boldsymbol{\delta}}_d,\boldsymbol{\gamma})$.

We follow Genest et al. (1995) who suggest to replace the estimation of marginals parameters estimation by non-parameteric estimation. Given non-parametric estimator $\hat{F}_i$ of the margins F_i, the estimator of the dependence parameters $\boldsymbol{\gamma}$ is

$$\hat{\boldsymbol{\gamma}} = \underset{\boldsymbol{\gamma}}{\operatorname{argmax}} \sum_{i=1}^{n} \boldsymbol{c}\{\hat{F}_{X_1}(x_{i,1}), ..., \hat{F}_{X_d}(x_{i,d}); \boldsymbol{\gamma}\}.$$

Both the simulated method of moments and the maximum likelihood estimation are unbiased. The question is which procedure is more suitable for hedging, especially given the fact that for CC's the overall hedge performance may be driven by tail risks.

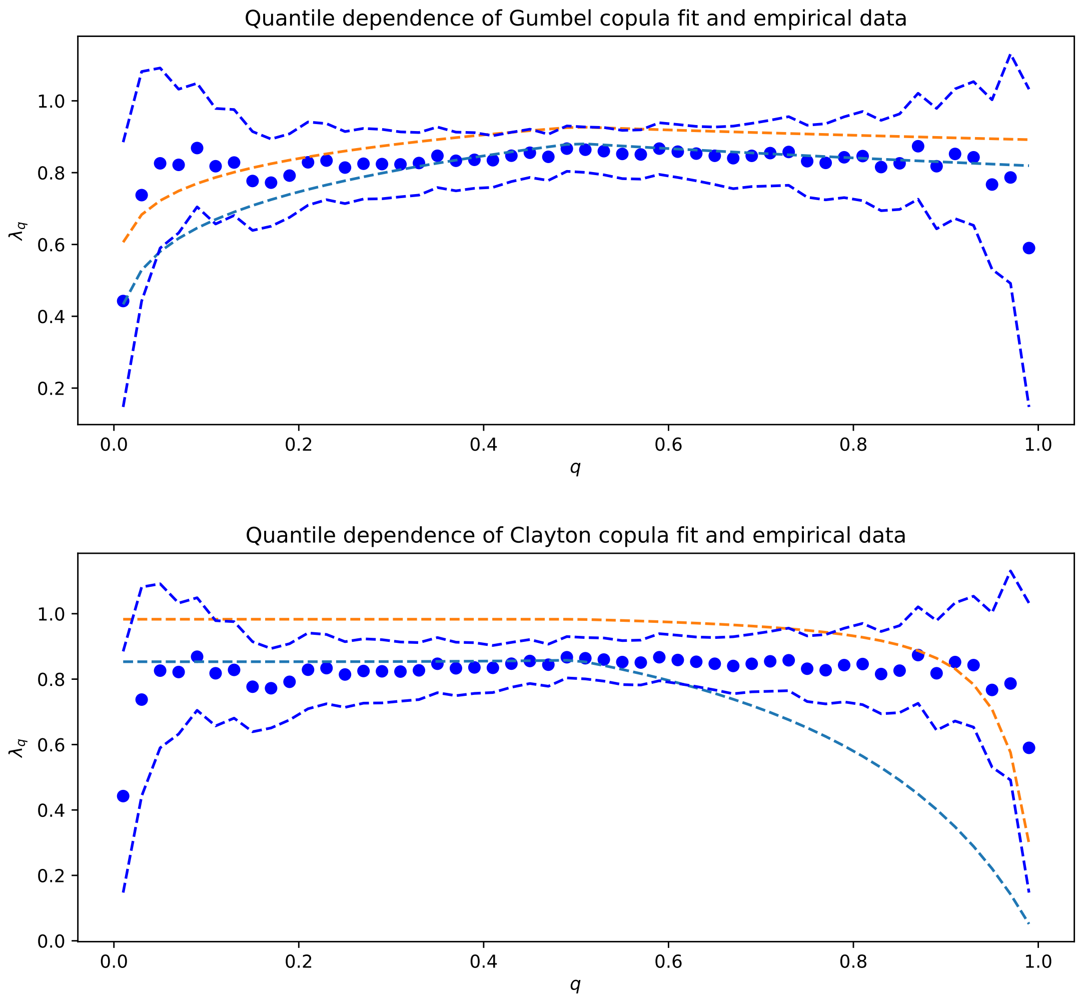

Figure 2: Quantile dependences of Gumbel and Clayton copulas. The blue circle dots are the quantile dependence estimates of Bitcoin and CME future, the blue dashed lines are the estimates' 90% confidence interval. The orange dotted line is the copula implied quantile dependence by MM estimation. The light blue dotted line is the copula implied quantile dependence by MLE estimation.

Figure 2 shows the empirical quantile dependence of Bitcoin and CME future and the copula implied quantile dependence of the MLE and MM calibration procedures. Although the MLE is a better fit to a range of quantile dependence in the middle, it fails to address the situation in the tails. We find that empirically the data has low quantile dependence in the lower ends ($q < 10\%$). *[How does the last sentence fit into the argument? Not sure I get it.]* Due to the better fit of the tail dependence structure, we choose MM as the calibration method. (was: We argue that MM is preferred as it produces a better fit to the dependence structure in the tail behaviour, contrary to MLE. Therefore, we deploy the method of moments throughout the analysis.) *[delete, this has been said already.] (was: We choose the 5^{th}-, 10^{th}-, 90^{th}-, 95^{th}-quantile, and Spearman's ρ as the moments.)*

3.2.3 Copula selection

As the (was: The) dependence structure of price data changes across time, (delete: in which both the dependency parameters and the type of dependence. For this reason,) we allow for a flexible choice of the best-fitting copula, by re-calibrating periodically and re-evaluating performance of the various copulas. In each re-calibration, we (was: We) select the best-fitting copula, characterised by the lowest *Akaike Information Criterion (AIC)*,

$$\mathrm{AIC} = 2k - 2\log(L),$$

where k is the number of estimated parameteres and L is the likelihood (Akaike, 1973).

Other model selection criteria, such as the TIC (Takeuchi, 1976) or likelihood ratio test could be used instead. For a survey of model selection and inference, see Anderson et al. (1998). Among various copula selection procedures, AIC is a popular choice for its applicability, see e.g. Breymann et al. (2003). In our case, the AICs are calculated only with dependence likelihood since the marginals are modelled via kernel density estimators. The selected copula will then enter the calculation of the optimal hedge ratio.

3.3 Risk measures

The optimal hedge ratio is determined for the following variety of risk measures: variance, Value-at-Risk (VaR), Expected Shortfall (ES), and Exponential Risk Measure (ERM). A summary of risk measures being used in portfolio selection problem can be found in Härdle et al. (2008). The risk measures here serve as risk minimization objectives, i.e. loss functions for searching the optimal hedge ratio.

The risk measures are defined as follows. Let Z be a random variable with distribution function F_Z.

1. Variance: $\mathrm{Var}(Z) = \mathbb{E}[(Z - \mathbb{E}Z)^2]$.
2. VaR at confidence level α: $\mathrm{VaR}_\alpha(Z) = -F_Z^{(-1)}(1-\alpha)$
3. ES at confidence level α: $\mathrm{ES}(F_Z) = -\frac{1}{1-\alpha}\int_0^{1-\alpha} F_Z^{(-1)}(p)dp$
4. ERM with Arrow-Pratt coefficient of absolute risk aversion k:

$$\mathrm{ERM}_k(F_Z) = \int_0^{1-\alpha} \phi(p) F_Z^{(-1)}(p)dp,$$

where ϕ is a weight function described in (3.3) below.

VaR, ES, and ERM fall into the class of spectral risk measures (SRM), which have the form (Acerbi, 2002)

$$\rho_\phi(r^h) = -\int_0^1 \phi(p) F_Z^{(-1)}(p)dp,$$

where p is the loss quantile and $\phi(p)$ is a user-defined weighting function defined on $[0,1]$. We consider only so-called admissible risk spectra $\phi(p)$, i.e., fulfilling

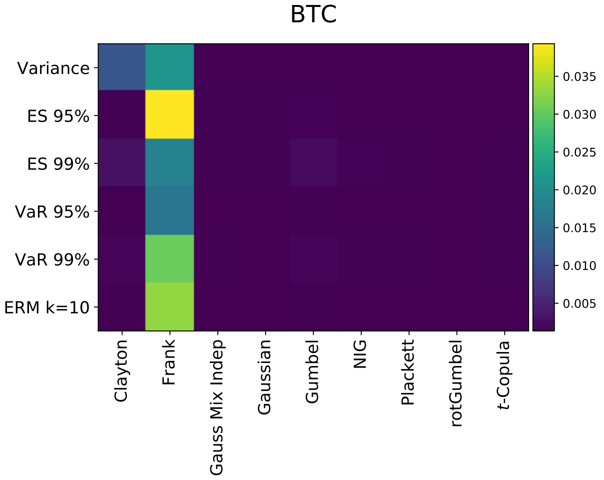

Figure 3: Out-of-sample mean square errors of BTC-BTCF portfolios constructed with different copula and risk minimization objectives. The Frank copula is inferior in the BTC-involved portfolios.

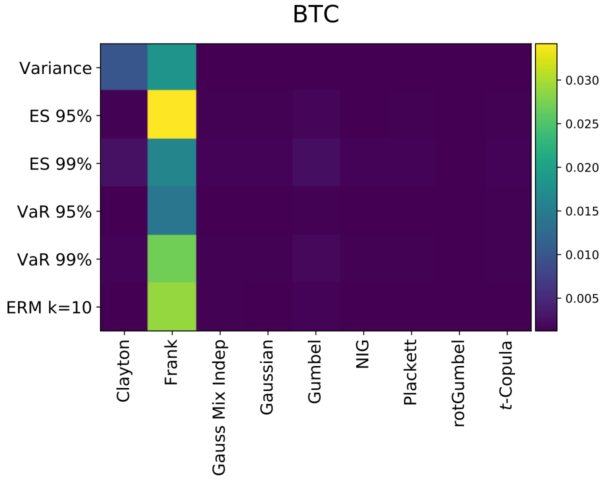

Figure 4: Out-of-sample lower semivariance of BTC-BTCF portfolios constructed with different copula and risk minimization objectives. The Frank copula is obviously inferior.

(i) ϕ is positive,

(ii) ϕ is decreasing,

(iii) and $\int \phi = 1$.

The VaR's $\phi(p)$ gives all its weight on the $1-\alpha$ quantile of Z and zero elsewhere, i.e., the weighting function is a Dirac delta function, and hence it violates the (ii) property of admissible risk spectra. The ES' $\phi(p)$ gives all tail quantiles the same weight of $\frac{1}{1-\alpha}$ and non-tail quantiles zero weight. The ERM assumes investors' risk preference are in the form of an exponential utility function $U(x) = 1 - e^{kx}$, so its corresponding risk spectrum is defined as

$$\phi(p) = \frac{ke^{-k(1-p)}}{1-e^{-k}},$$

where k is the Arrow-Pratt coefficient of absolute risk aversion. The parameter k has an economic interpretation as being the ratio between the second derivative and first derivative of investor's utility function on an risky asset,

$$k = -\frac{U''(x)}{U'(x)},$$

for x in all possible outcomes. In case of the exponential utility, k is the the constant absolute risk aversion (CARA).

4 Empirical Results

4.1 Data

In the empirical analysis, we consider the capability (was: the risk reduction capability) of CME Bitcoin Futures (BTCF) to reduce the risk of (was: on) five cryptos, namely Bitcoin (BTC), Ethereum (ETH), Cardano (ADA), Litecoin (LTC) and Ripple (XRP), as well as five crypto indexes, namely BITX, BITW100, CRIX, BITW20 and BITW70. The currencies ETH, ADA, LTC, and XRP are popular cryptos traded at various exchanges and have large market capitalization. BITX, BITW100, and CRIX are market-cap weighted crypto indexes with BTC as constituent. BITX and BITW100 track the total return of the 10 and 100 cryptos with largest market-cap, respectively. CRIX determines the number of constituents via AIC and tracks this number of cryptos with largest market-cap. In our case, the number of constituents in the CRIX is 5. BITW20 is also a market-cap weighted crypto index but with the 20 largest market-cap cryptos outside the constituents of BITX. BITW70 has the same construction as BITW20 but with the 70 largest market-cap cryptos outside BITX and BITW20. Therefore, BTC is excluded as a constituent in BITW20 and BITW70.

For each of the ten hedge portfolios, a crypto or index is considered as the spot and held in a unit size long position, while the front BTCF is held in a short position with units corresponding to the optimal hedge ratio in order to reduce the risk of the spot. Except for the hedge of BTC, all hedging portfolios are considered to be cross-asset hedges.

[What is the whole time frame?]

We collect the spots' and BTCF's daily prices at 15:00 US Central Time (CT). The reason for choosing this particular time is that the CME group determines the daily settlements for BTCF's based on the trading activities on CME Globex between 14:59 and 15:00 CT. This is also the reporting time of the daily closing price by Bloomberg. The crypto spot data is collected from the data provider called Tiingo (https://www.tiingo.com/). Tiingo aggregates crypto OHLC (open, high, low, and close) prices fed by APIs from various exchanges. It covers major exchanges, such as Binance, Gemini, Poloniex, so Tiingo's aggregated OHLC price is a reasonable representation of a tradable market price. For each crypto, we match the opening price at 15:00 CT from Tiingo with the daily BTCF closing price from Bloomberg. Since CRIX is not available at 15:00 CT, we recalculated an hourly CRIX using the monthly constituents weights and the hourly OHLC price data collected from Tiingo. BITX, BITW20, BITW70, and BITW100 are collected from the official website of their publisher Bitwise.com. The daily reporting time of the Bitwise indexes is 15:00 CT.

At the time of writing, the CRIX is undergoing the listing process on the S&P Dow Jones Indices. The official CRIX data will then be calculated with Lukka Prime Data and available to the public via S&P. *[Is this still the case?]*

4.2 Overview of the out-of-sample data

The date range of the out-of-sample time series is from 2019-10-21 to 2021-05-27, in total of 405 data points in each time series. For every asset and hedge portfolio, we concatenate the out-of-sample data to form a time series for analysis. We analyse this time series throughout the whole result section. *[Either mention the time range of the in-sample data or mention the whole data range above, where it is specified that the data are from 15.00 each day, etc.]*

We introduce the out-of-sample data in this subsection before we proceed to analysing the hedged portfolio results. Figure 5 presents the BTC and BTCF price in USD in the first panel and the difference between the daily returns of BTC and BTCF, i.e. $R_s - R_f$, in the second panel. In the first panel, the black vertical lines with capital letters labels indicate the days of the five most negative daily BTC returns during out-pf-sample period. Table 1 summarizes the relevant news headlines and events of those days.

Figures 6 and 7 show the cumulative returns of the indices and individual cryptos, respectively. The vertical lines labeled by assets name refer to the largest daily price drops of each asset in the out-of-sample data.

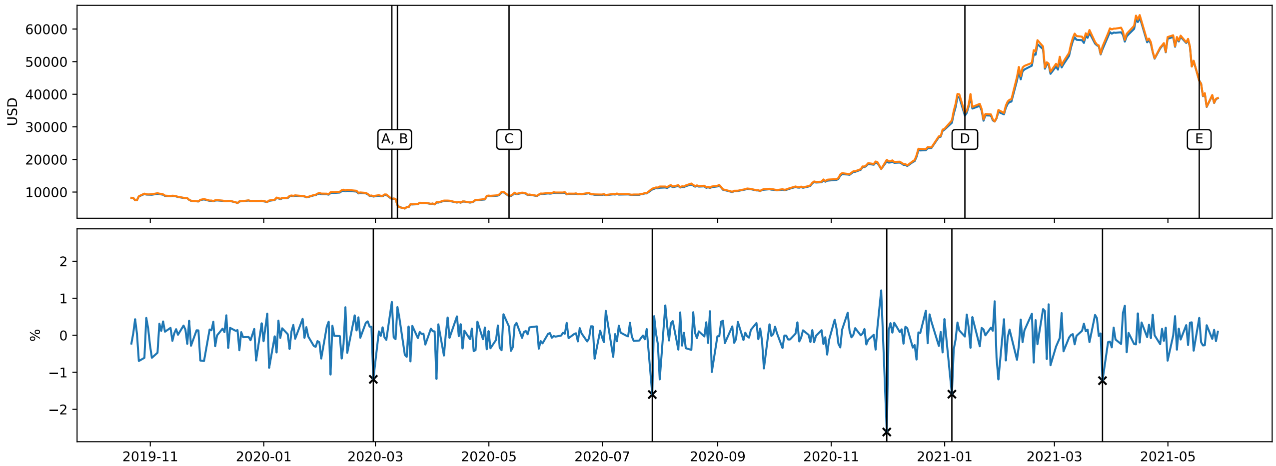

Figure 5: Out-of-sample BTC and BTCF price. The first panel presents the price of BTC in blue line and that of BTCF in orange line. The black vertical lines with capital letter labels indicate the five most negative daily return of BTC in the out-of-sample data. The second panel presents the difference between the percentage returns of BTC and BTCF. The black vertical lines indicate the five most negative returns. The crosses locate the level the returns.

The out-of-sample data covers the pre-COVID19 period, 2019-10-21 to 2020-03-09, as well as the COVID19 period, 2019-03-19 onwards. We can observe an overall upward trend of crypto prices in both periods. Nonetheless, the volatilities of assets are high (annualized around 100%) regardless of COVID19.

Label	Date	% Drop in Price	Summary
A	2020-03-09	13.83	Coronavirus outbreak that affects the global markets; BTC as potential safe-haven was questioned.[1]
B	2020-03-12	22.89	Continuation of the 2020-03-09 drop.
C	2020-05-11	12.11	Price correction (from \$10,000 to \$8,100) after BTC price surge because of the third supply halving.[2,3]
D	2021-01-11	14.41	Short term correction of BTC hits the \$40,000 mark.[4]
E	2021-05-17	11.86	Tesla stops accepting BTC as payment currency due to environmental concerns related to the excessive energy use in processing transactions.[5]

Table 1: Summary of events associated with the five most extreme daily price drops in out-of-sample BTC price data. The capital letter labels in the first column correspond to the labels in the first panel of figure 5. [1] is reported by the CNBC news `https://cnb.cx/3HZ2x7K`; [2] is from Forbes `https://bit.ly/3rdJPmP`; [3] is from livemint.com `https://bit.ly/3FRi6Na`; [4] is from CNBC `https://cnb.cx/3nU0pp0`; [5] is from Reuters `https://reut.rs/3leCiAv`.

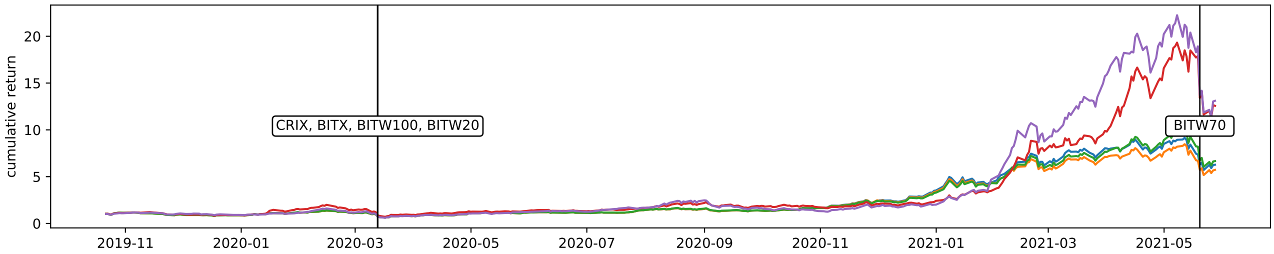

Figure 6: Out-of-sample cumulative returns of crypto indices. The black vertical lines indicate the largest price drops of each index as indicated by the labels. The colouring is as follows: Blue line is CRIX; Orange line is BITX; Green line is BITW100; Red line is BITW20; Purple line is BITW70.

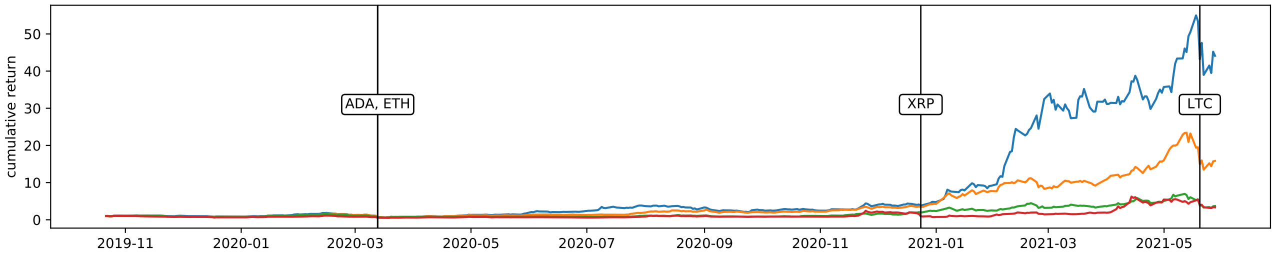

Figure 7: Out-of-sample cumulative returns of individual cyptos. The black vertical lines indicate the largest price drops each cryptos as indicated by the labels. Blue line is ADA; Orange line is ETH; Green line is LTC; Red line is XRP.

Label	Date	% Drop in Price	Summary
CRIX	2020-03-09	23.77	Coronavirus outbreak that affects the global markets including the crpyto market.
BITX		23.68	
BITW100		23.87	
BITW20		26.66	
ADA		23.55	
ETH		27.40	
BITW70	2021-05-19	27.64	Spillover of the BTC shock on 2021-05-17 (label A in Figure 5 and Table 1)
XRP	2020-12-23	41.00	Top executives of Ripple Labs sued by the SEC of misleading investors[1].

Table 2: Summary of events that associated with largest price drops in out-of-sample data. The labels in the first column are the labels in figure 6 and figure 7. CRIX, BITX, BITW100, BITW20, ADA and ETH have the same date the reason of the largest drop.[1] is reported by Bloomberg `https://bloom.bg/3cWdita`.

[Table 2 is not referenced in the text. Please fix.]

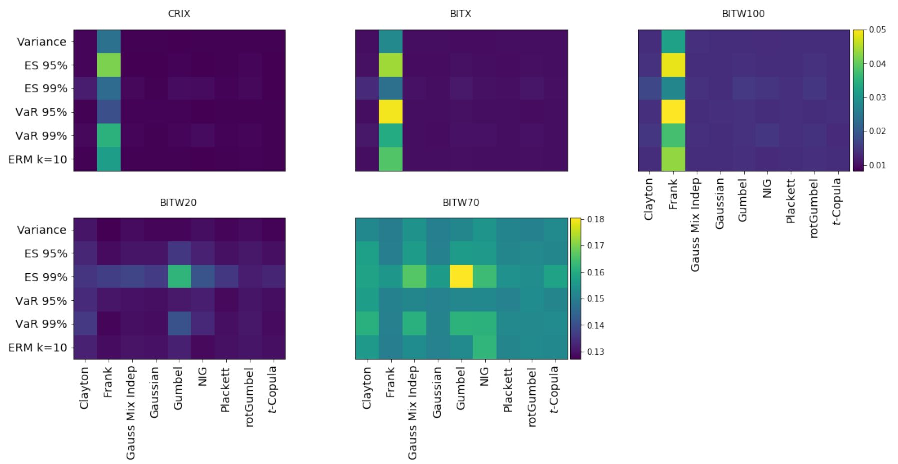

Figure 8: Out-of-sample mean square errors of indices' hedge portfolios. Plots in a row share the same colour scale for comparison.

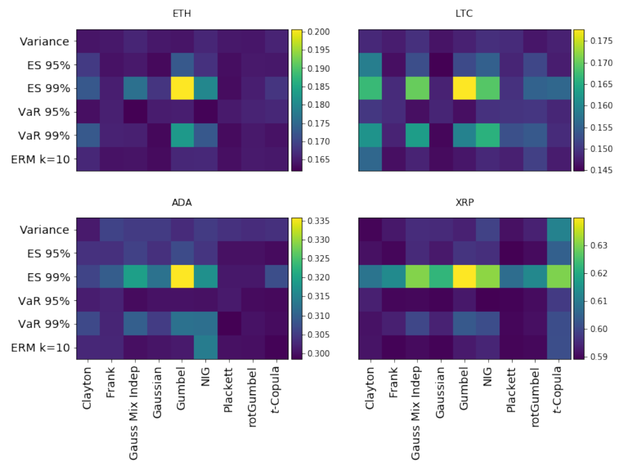

Figure 9: Out-of-sample mean square errors of cryptos' hedge portfolios. Each plot has its own colour scale.

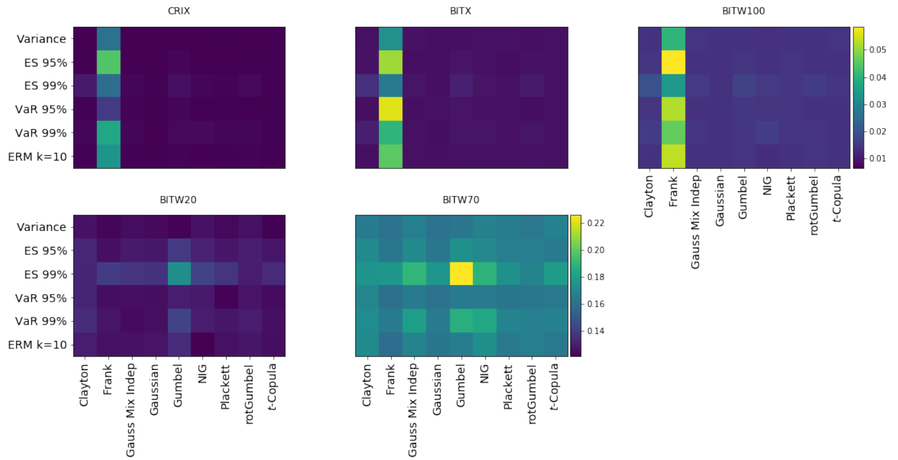

Figure 10: Out-of-sample lower semi variance of indices' hedge portfolios. Plots in a row share the same colour scale for comparison.

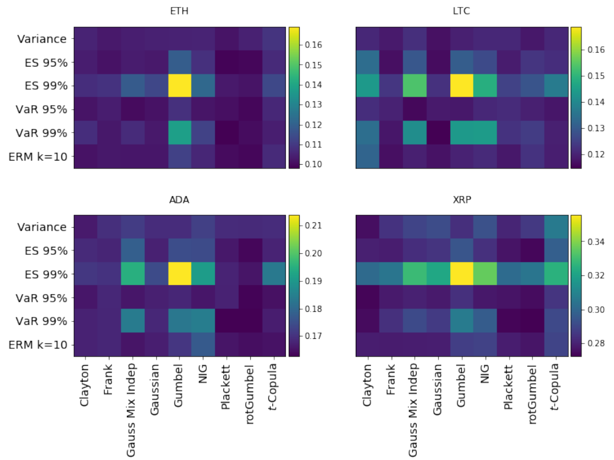

Figure 11: Out-of-sample lower semi variance of cryptos' hedge portfolios. Each plot has its own colour scale.

4.3 An overview of the hedged portfolios without the copula selection step

First, we analyse the results of the hedged portfolios without the copula selection step in order to get a better understanding of how a copula affects the hedged portfolio with various risk minimization objectives. To do so, we inspect the hedge performance of copulas by the mean square error and lower semi-variance. The mean square error is the distance between a perfect hedge and the hedged portfolio returns $\text{MSE} = \mathbb{E}(R^2)$. The lower semi-variance is defined as $\text{LSV} = \mathbb{E}\left((R - \mathbb{E}(R))^2 \mathbf{1}_{\{R \leq \mathbb{E}(R)\}}\right)$. All results presentedd here are out-of-sample results obtained without the copula selection step in order to compare the performances across copulae.

[Please fix order of figures and references. Figures 3 and 4 are referenced here for the first time, when Figures 5 etc. have already been discussed in the previous section.]

Figure 3 and 4 are the mean square error and lower semivariance of BTC-BTCF. By far, the Frank copula is the worst performing copula. In Figures **??** and **??**, the phenomenom of the Frank copula being inferior to its counterparts can be observed for the CRIX, BITX, BITW100, and BITW20-BTCF portfolios. Interestingly, in all of these portfolios, the spot has a strong dependence with the BTCF. In contrast, the inferiority of the Frank copula is less prominent in the BITW70, ADA, ETH, LTC and XRP-BTCF portfolios. As a consequence, it appears that the Frank copula is not an appropriate choice to model assets with strong dependence.

A further observation from Figures **??** and **??** is that the Gumbel copula does not perform as well as other copulas in the ETH, LTC, and XRP-BTCF portfolios. The reason is that the Gumbel copula has only upper tail dependence, while ETH, LTC, and XRP exhibit lower tail dependence with BTCF. We shall discuss this in the following section.

[Please also reference the lower semi-variance figures. All figures and tables must be reference. Is it possible to increase the font sizes in the graphs, at least for the titles. They will not be readable in the final version otherwise. Also – as mentioned before – please create .eps or .pdf graphics. These are scalable, wheres png does not scale well.]

4.4 Copula Selection Results

Next, we inspect the copula selection results by the AIC procedure described in section 3.2.3. Although the copula selection is only an intermediate step to obtain the optimal hedge ratios, the result of this step can help us better understand the dependence feature between BTCF and the assets we study in this work. This provides valuable information for modeling the assets in the future. The decisions of the AIC procedure are summarised in Table 3. Overall, the t-copula, rotated Gumbel (rotGumbel), and the NIG factor copula are the most frequently chosen copulae by the AIC procedure.

The t-copula is predominantly to model the dependence between the BTC and BTC-involving-indices, CRIX, BITX, BITW100, and the BTC future. BTC and BTC-involving-indices exhibit strong (upper and lower) tail dependence with BTCF. We interpret tail dependence as a strong tendency for one asset to be extreme when the other is extreme and vice versa (McNeil et al., 2015). In fact, the t copula has been recommended in various empirical studies to model financial data, such as Zeevi and Mashal (2002) and Breymann et al. (2003). Those studies suggest that the t-copula is a better model compared to the Gaussian copula as financial data typically exhibit heavy tails and tail dependence.

[I do not understand the argument with the radial symmetry. Specifying the definition of radial symmetry is also not helpful here. To sharpen the argument, it should be something like this: On the other hand, the symmetry of the t-copula appears to be a poor choice to model the remaining hedging pairs. Here, the AIC criterion predominantly selects copulas that allow for asymmetry between the spot

Spot/ Copula	t	Plackett	GMI	rotGumbel	NIG
Individual Cryptos					
BTC	73	4	2	1	31
ETH	3	6	8	94	1
ADA	0	0	0	0	112
LTC	13	0	3	32	64
XRP	0	31	3	78	0
Crypto Indices with BTC Constituent					
BITX	39	0	14	16	12
CRIX	47	0	11	3	27
BITW100	42	0	8	29	2
Crypto Indices without BTC Constituent					
BITW20	0	0	0	78	3
BITW70	0	0	0	80	1

Table 3: Copula selection results (shortened). The values are the absolute frequencies of a copula chosen by the AIC procedure during the out-of-sample period. Each frequenc represents five trading days, which corresponds to the recalibration interval. The table show the frequently chosen copulas, which are t, Plackett, Gaussian Mix Independent (GMI), rotated Gumbel (rotGumbel) and Normal Inverse Gaussian factor copula (NIG).

and the underlying. This reflects that overall dependence between a non-BTC-related spot asset and the BTCF may be low, but tail risk, especially on the down-side is present, as crashes in the crypto market, which occur frequently, do not differentiate between assets.] On the other hand, the *(delete: radial)* symmetry of the t-copula appears to be a poor choice to model the remaining hedging pairs. Demarta and McNeil (2005) describes the radial symmetry feature of the t-copula "strong" as it is a radially symmetric distribution. To be specific, if $(U_1, ..., U_d)$ is a vector distributed in t-copula, then $(U_1, ..., U_d) \stackrel{\mathcal{L}}{=} (1-U_1, ..., 1-U_d)$. This symmetry can be justified in the dependence structure between a futures and its underlying by the theory of futures pricing, which suggests the price of a futures is a function of the underlying price (Hull, 2003). However, there is no such relationship between a futures and an asset which is not the underlying. Besides, asset prices tend to crash simultaneously whereas positive development tends to be idiosyncratic.

Among the three popular copulae, rotGumbel copula shows its ability to model the dependence between ETH and BTCF. rotGumbel also performs well when modelling dependence between XRP, BITW20, BITW70, and the BTCF. In particular, the whole time series of the two indices, BITW20 and BITW70, are best fitted solely with the rotated Gumbel copula.

In fact, Clayton's AIC in many of the training sets is the second lowest, just higher than that of rotated Gumbel. This is because the Clayton copula has the same ability to model the lower quantile dependence. However, Clayton's radial like feature does not match the behaviour of the financial data.

It is worth to mention that although the NIG factor copula is penalised heavily due to its three parameters setup, it is frequently chosen to be the best copula to model the dependence between individual cryptos and the BTC future. An extreme case would be ADA, where only the NIG factor is chosen in our dataset. Another dependence structure best described by the NIG factor copula is the pair of LTC-BTCF, with 64 out of 112 training sets best fitted by the NIG factor copula. Indices like BITX and CRIX are sometimes best fitted with the NIG factor copula as well, accounting for modelling 12 and 27 training sets, respectively. The popularity of the NIG factor copula reflects the ability of the copula to model complex dependence structure, involving heavier tails than the Gaussian as well as asymmetric distributions. (was: the NIG factor copula is able to model the tail, radial asymmetry.)

The Frank copula turn out to generally be a poor choice to model financial data (as also reported by Barbi and Romagnoli (2014)). The Plackett copula is characterised by its dependence parameter being equal to the cross-product ratio, see eq. 9. However, apparently, this property does not capture the dependence structure of cryptos and BTCF.

4.5 Hedged portfolios with the copula selection step

We now turn to the hedge performance. Table 4 presents the first two moments, maximum drawdown (MD) and the date of MD of the hedge portfolios. An interesting observation is the similarity of the statistics when minimising with respect to different risk measures. (was: We observe that the statistics of the portfolios with different objectives are similar to each other. *[Unclear what is meant by "different objectives"? Different risk measures?]*) Detailed statistics are found in Tables 6 to 11 in Appendix C.

Unsurprisingly, the BTC-involved spots, i.e., BTC, CRIX, BITX, and BITW100, are well hedged by the BTCF regardless of risk minimization objective. The BTC-not-involved spots, on the contrary, are less promising. Those hedge portfolios' returns are as volatile or nearly as volatile as the assets themselves, see for example ADA and XRP. We shall further discuss the effectiveness of hedge in the next section.

4.6 Hedging Effectiveness Results

In this section, we analyse the out-of-sample hedging effectiveness (HE) of BTCF as a hedge instrument. HE is defined as

$$\mathrm{HE} = 1 - \frac{\rho_h}{\rho_s},$$

i.e., it measures the percentage reduction of risk of the hedge portfolio ρ_h relative to the risk of the spot position ρ_s. A higher HE indicates a greater risk reduction and thus the hedge is more effective. The HE above is a generalisation of how Ederington (1979) evaluates hedge performance, which focusses on variance as the risk measure. Aside from variance, we include the risk measures which act as loss function while searching for the optimal hedge ratios: ES 95% and 99%, VaR 95% and 99% and ERM.

[A description is missing of how the hedge actually works. How much data enters the calibration (I believe it's 300 days). Then what happens? On each day we have a hedge ratio. Do we construct a new hedge each day? How long is the hedge period? So, after which time period is P&L calculated. This could also be added to Section 2.2.
What is the motivation behind the bootstrapping?]

The formulation above gives a point estimate per test data point (was: testing data). However, each of our test data contain only 5 data points, the length is not sufficient to draw meaningful risk measure results. *[Last sentence unclear, because information is missing, see above.]* To address this issue, we apply bootstrapping method on the concatenated test data time series as described in the beginning of the result section.

Bootstrapping refers to sampling from the empirical distribution of a given data sample (e.g. a time series of fiancial returns). The principal idea underlying bootstrapping is to provide statistical information about estimators that cannot be derived from just one realisation of the data. The method was introduced by Efron (1979); see also (Efron and Tibshirani, 1994; Davison and Hinkley, 1997).

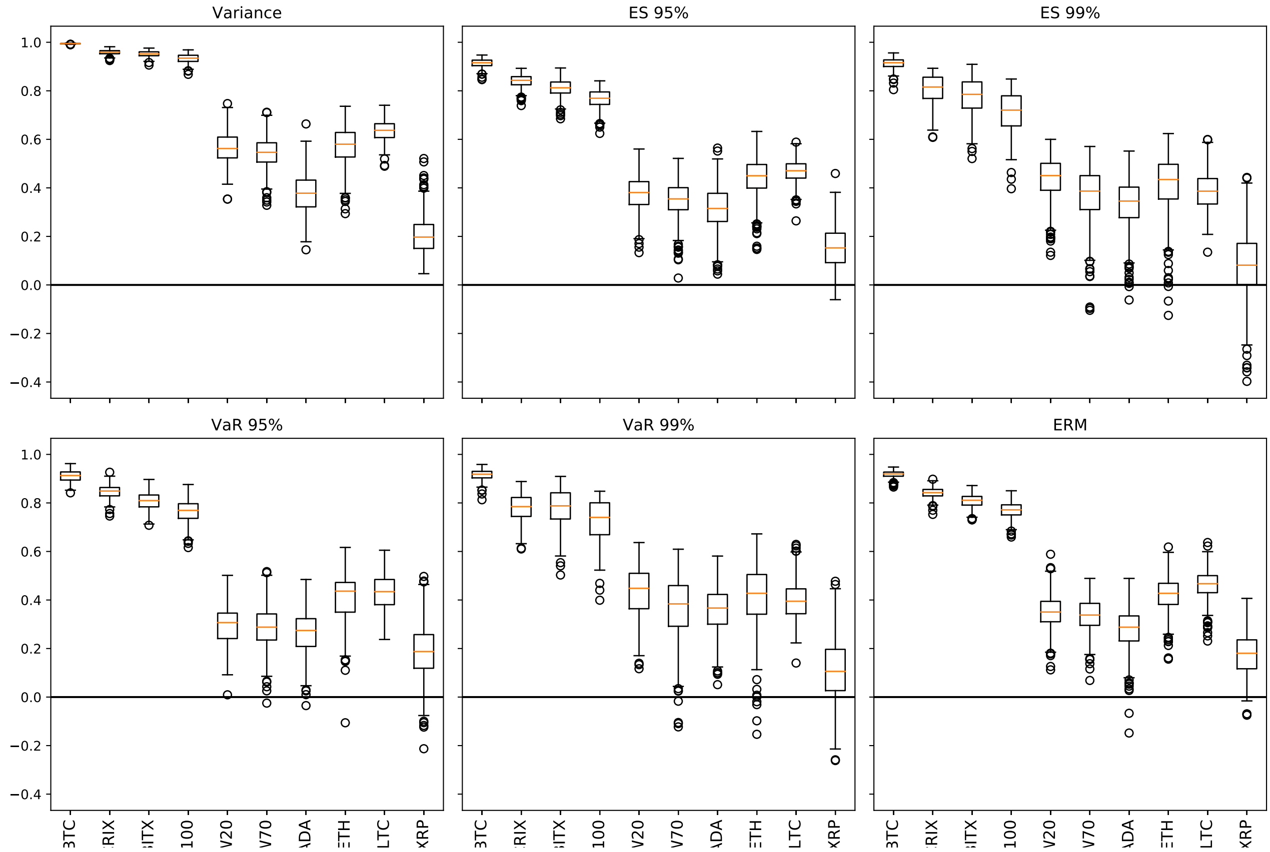

Figure 12: Hedging effectiveness (HE) of portfolios with different risk minimization objectives evaluated by the corresponding risk minimization objectives. The boxplots indicate the the median, upper quartile, lower quartile, minimium and maximum of the bootstrapped HE. The HE of BTC-involved spots are significantly higher than that of BTC-not-involved spots.

	BTC	ETH	ADA	LTC	XRP	BITX	CRIX	BITW100	BITW20	BITW70
Assets										
Mean %	0.3915	0.6819	0.9467	0.3227	0.2987	0.4308	0.4602	0.4683	0.6249	0.6353
Std %	4.4023	6.0103	6.699	6.4781	7.9843	4.5676	4.542	4.6174	5.5021	5.8155
MD %	-25.9965	-32.0144	-26.8528	-37.5913	-52.7652	-27.022	-27.1385	-27.2694	-31.0092	-32.3453
MD date	2020-03-12	2020-03-12	2020-03-12	2021-05-19	2020-12-23	2020-03-12	2020-03-12	2020-03-12	2020-03-12	2021-05-19
Variance minimizing portfolios										
Mean %	0.0215	0.2823	0.5617	-0.0871	-0.0123	0.0561	0.0812	0.0855	0.2429	0.2706
Std %	0.3221	3.8741	5.2722	3.9052	7.1537	0.9954	0.9183	1.1986	3.5846	3.8838
MD %	-1.4393	-17.7421	-13.8687	-28.3029	-52.5236	-7.7567	-7.1025	-11.3866	-21.468	-23.9984
MD date	2020-11-30	2021-05-19	2021-01-08	2021-05-19	2020-12-23	2021-05-19	2021-05-19	2021-05-19	2021-05-19	2021-05-19
VaR 95% minimizing portfolios										
Mean %	0.0253	0.3084	0.5726	-0.0742	0.0208	0.0562	0.0863	0.0846	0.2728	0.2847
Std %	0.3294	3.8944	5.2204	3.9145	7.152	0.993	0.9151	1.198	3.594	3.9133
MD %	-1.5347	-19.175	-14.6974	-28.3672	-52.5667	-7.5639	-6.9744	-11.2582	-22.0733	-24.6513
MD date	2020-11-30	2021-05-19	2021-05-19	2021-05-19	2020-12-23	2021-05-19	2021-05-19	2021-05-19	2021-05-19	2021-05-19
VaR 99% minimizing portfolios										
Mean %	0.0176	0.2977	0.5562	-0.0852	0.0352	0.0593	0.0738	0.0823	0.2499	0.2788
Std %	0.3270	3.9132	5.3466	4.1503	7.1658	1.0178	0.9695	1.2338	3.621	3.9257
MD %	-1.5689	-18.6061	-15.4795	-29.0915	-52.5727	-8.0299	-7.0185	-11.8752	-21.6634	-24.5294
MD date	2020-11-30	2021-05-19	2021-05-19	2021-05-19	2020-12-23	2021-05-19	2021-05-19	2021-05-19	2021-05-19	2021-05-19
ES 95% minimizing portfolios										
Mean %	0.0204	0.3082	0.5525	-0.0808	0.0176	0.0591	0.0777	0.0848	0.2608	0.2785
Std %	0.3234	3.889	5.2673	3.9829	7.1533	1.0065	0.9207	1.2125	3.6115	3.9157
MD %	-1.5629	-18.7819	-14.9647	-28.4608	-52.5698	-7.6211	-6.9894	-11.1357	-21.543	-24.3474
MD date	2020-11-30	2021-05-19	2021-05-19	2021-05-19	2020-12-23	2021-05-19	2021-05-19	2021-05-19	2021-05-19	2021-05-19
ES 99% minimizing portfolios										
Mean %	0.0148	0.308	0.5016	-0.1029	-0.02	0.0598	0.0835	0.0781	0.2538	0.266
Std %	0.3476	3.8954	5.404	4.1581	7.2887	1.0312	0.9461	1.264	3.6323	3.932
MD %	-1.6225	-18.7625	-15.4481	-29.1727	-52.57	-7.7424	-7.0203	-11.9263	-21.9866	-24.4764
MD date	2020-11-30	2021-05-19	2021-05-19	2021-05-19	2020-12-23	2021-05-19	2021-05-19	2021-05-19	2021-05-19	2021-05-19
ERM $k = 10$ minimizing portfolios										
Mean %	0.0223	0.3117	0.5722	-0.0512	0.0155	0.059	0.084	0.0853	0.2564	0.2818
Std %	0.3221	3.8679	5.359	3.8812	7.1579	1.0078	0.9087	1.2032	3.6009	3.9074
MD %	-1.5242	-18.8729	-14.3885	-28.0879	-52.5689	-7.8581	-7.053	-11.1846	-21.592	-24.525
MD date	2020-11-30	2021-05-19	2021-01-08	2021-05-19	2020-12-23	2021-05-19	2021-05-19	2021-05-19	2021-05-19	2021-05-19

Table 4: First two moments, maximum downdown (MD) and date fo MD of assets and hedge portfolios out-of-sample return.

(was: The bootstrapping method is known to be a powerful nonparametric tool for approximating complicated statistics (Efron and Tibshirani, 1994; Davison and Hinkley, 1997).)

We apply the stationary block bootstrap of Politis and Romano (1994) in our analysis in order to account for the time-dependence of the data while sampling. The sampling method of the stationary bootstrapping procedure is as follows. Assuming a time series $\{X_t\}_{t\in[1,N]}$ that is a stationary strong, weakly dependent time series. Blocks of samples $\{X_i, ..., X_{i+j-1}\}$, where the index i is a random variable uniformly distributed over $[1, 2, ..., N]$ and j is geometric distributed random variable with parameter p independent of i. For any index k which is greater than N, the sample X_k is defined to be $X_{k(\mod N)}$. *[Fix notation with* mod *operator.]* For each block, we calculate the hedging effectiveness as outlined above. We choose $p = 1/250$, implying the average block length is 250. *[I think this was changed, right?]* This average block length is chosen to reasonably calculate ES and VaR. 100 blocks are drawn for each risk minimising objective and spot.

[The previous part still needs quite a bit of work as it remains unclear to the reader what is actually going on. The principal idea is to create an out-of-sample distribution of HE, but with one sample path this is not possible. Therefore, the bootstrap, right?]

Figure 12 report the bootstrapped HE samples from the concatenated out-of-sample hedge portfolio return. As expected, the BTC involving spots, the BTC, CRIX, BITX and BITW100, are well hedged by the BTCF. The HEs of the other cryptos and indices are substantially lower than to the BTC-related instruments, but exhibit a consistent performances across different risk measures. As it turns out, some HE bootstrapping samples are even negative, which means the "hedge" portfolio actually increases the risk. This is, of course, counter-productive to hedging indicating that BTC futures may not be suitable for cross-asset hedges (was: This is an unfavorable situation for investors if they want to hedge cryptos with BTC futures. We do not recommend BTC futures being used to cross hedge cryptos.)

5 Conclusion and Outlook

We study the effectiveness of hedging cryptos and crypto indices with Bitcoin futures. To accomodate different risk appetites and scenarios, a variety of commonly used risk measures are considered to determine the optimal hedge ratio. The risk measures comprise variance, value-at-risk at the confidence levels 95% and 99%, expected shortfall 95% and 99%, and the exponential risk measure with parameter $k = 10$.

At the time of writing, the crypto market is a vibrant and fast-developing market, causing cryptos to have complex and time-changing dependence structures with the Bitcoin futures. As a consequence, the dependence between the cryptos and the futures contract plays an important role in hedging as it determines the distribution of the portfolio returns. We therefore consider various copulae, a flexible statistical tool that separates modelling of the marginals and the dependence structure of multivariate random vectors. To address the potential time-changing dependence, we periodically re-calibrate the copula models and determine the best-fitting copula via AIC.

An extensive out-of-sample backtest suggests that Bitcoin futures are consistently capable of hedging BTC and BTC-involved indices, i.e., BITX, CRIX, and BITW100, under different risk minimisation objectives and copula models. The mean-square errors (MSEs) and lower semi-variances (LSVs) of the resulting portfolios are indistinguishable at a low level except for the Frank copula. For BTC-related spot asset, the AIC procedure consistently favours the t-copula because it captures the tail dependence feature of the data. Compared to the unhedged cases, the portfolios' out-of-sample maximum drawdowns are significantly reduced.

Contrarily, we observe more diverse results of the capability of BTC futures to hedge other cryptos and crypto indices that exclude Bitcoin. In general, ES 95% and VaR 95% perform better than their 99% counterparts. In particular, minimising ES 99% leads to relatively high MSEs and LSVs regardless of the copula in use. The ES 99% and VaR 99% even result in out-of-sample maximum drawdowns that are higher than that of the 95% counterparts in some portfolios, for example in the ETH- and LTC-BTCF portfolio. Therefore, we conclude that overly emphasising tail risks by choosing extreme tail risk measures does not lead to a promising hedge in a cross-hedging setting.

The AIC procedure mainly favours the rotated Gumbel and the NIG factor copula in modelling non-BTC relate cryptos and indices. This reflects the systematic (was: idiosyncratic) nature of downward movements in the crypto market. Interestingly, the best-fitting copula does not necessary lead to the best performing portfolio in terms of MSE or LSV. This is the case, for example, for ADA. We suspect that this discrepancy between the optimal copula selection and MSE-LSV results can be attributed to the static linear nature of the hedge, as the sole hedge instrument is a futures contract; the hedge is not sophisticated enough to react to the more involved dependence structure.

[Argh... why a new paragraph here? I suggest to delete the first sentence...] Although copulae are flexible to model complex dependence structures by emphasising a number of important features such as lower tail dependence and radial symmetry, the simple linear hedge is very limited in its flexibility to address this complex dependence. Including liquidly traded derivatives with non-linear payoffs, such as options, might be a possibility to improve the hedge quality for these cryptos and portfolios.

[The paper is finished after the conclusion! The discussion needs to be earlier.]

6 Discussion

[What is the goal of the discussion? If I remember correctly we wanted to mention that we use CME data as we have an institutional trader as a market maker in mind. This should go into the introduction. If you want to include policy makers, can you summarise this in a few sentences? Otherwise, we should leave this out, as we are not aiming at policy advice in this paper.]

Cryptohedgers: Our results and conclusion are drawn using a non-parametric way, kernel density estimation, to fit the marginal density of the crypto and futures returns because we intend to leave the modelling of marginal distributions flexible and generic. Copula provides the flexibility to model marginal distributions separately. That means the model assumption and parametrisation for spot and futures can be different. This empowers hedgers to make use of variety of statistical tools to model the marginal distributions according to asset specific features they are interested, to enhance the model predictability, and hence, to improve the hedging effectiveness. For example, one can use various types of GARCH to deal with clustered volatility observed from the spot while using structural time series to deal with seasonality in futures; alternatively, using Hawkes processes to deal with clustered jumps in spots and futures without modelling the spillover or co-jumps in the marginal distribution. Hedgers are allowed to be creative in this regard. In fact, many researchers have enriched the understanding of the crypto market dynamics, see for example Kaiser (2019), Gyamerah and Abaitey (2022), and Mark et al. (2022). Although the hedging effectiveness of combining various statistical tools with copula remain an open question, our analysis shows that hedgers have the freedom to choose the copula (except the Frank copula) to model the dependence structure, whereas t, Plackett, Gaussian Mix independent, rotated Gumbel and NIG copula appear to be conservative choices to start the analysis.

Policy makers: Our results connect to the discussion of minimum capital requirements for crypto market risk exposure. The Basel Committee on Banking Supervision (BCBS) has made proposals and released consultative documents for the prudential treatment of banks' crypto-asset exposures. The Basel chair's stand on placing tough capital rules for crypto assets [4] attracted discussion. The Second Consultation proposes to limit banks' exposures to Group 2 cryptoassets to 1% of the bank's Tier 1 capital, calculated on a "double-gross" basis by adding the long and short positions without any hedging recognition $\text{Net position} = \max(\text{Long position}, |\text{Short position}|) - .65 \min(\text{Long position}, |\text{Short position}|)$ (60.66). Respondents to the consultations argued that the proposed methodology of calculating exposure is an extremely restrictive quantitative measure that prohibits banks to manage limit utilisation to crypto assets as the addition of a hedge instrument; a price increase of the underlying cryptoassets could make banks breaching the limit. According to our results, BTC position's market risk measured in various risk measures, even for VaR99% and ES99%, can be effectively reduced by an appropriate size of opposite position in CME BTC futures. While the debates carry on at the time of writing, our results align and can be seen as an extension of the existing researches made by stakeholders, for example, research done by CME [5], and International Swaps and Derivatives Association's report [6].

On the other hand, our results support the cryptoassets categorisation criteria proposed by the Basel Committee. In the Second Consultation, Group 2 cryptoassets (Group 1 CCs are digitally tokenised traditional assets) are divided into two subcategories, Group 2a are the CCs that exists a derivative or exchange-traded fund (ETF)/exchange-traded note (ETN) that is traded on a regulated exchange that solely references the cryptoasset; Group 2b are the CCs that fail to meet the requirement. Our results suggest that the existence of derivative that solely references the cryptoasset empowers market participants to hedge their corresponding crypto position, thus it is sensible to treat the aforementioned Group 2a and 2b differently. On the contrary, we show that the hedging effectiveness significantly lower than 1 when the spot is different from what the CME futures is referencing, i.e. the cross hedge setting. That means the risk of holding a CC cannot be perfectly cross hedged by including the CME futures. Even worse, we observe negative HEs in some of the bootstrapped samples. From the great difference in hedging effectiveness between the BTC-BTCF and other cross hedge portfolios, we conclude that the existance of derivative that solely reference the cryptoasset is a sensible choice of crtyptoassets categorisation criteria as it reflects assessibility of market participants to form risk reduction strategy.

[4]See https://www.risk.net/regulation/7948536/basel-chair-stands-by-tough-capital-rules-for-crypto-assets

[5]See the CME and KPMG's report on https://www.cmegroup.com/education/files/basics-of-hedge-effectiveness.pdf

[6]See the ISDA report "Crypto-asset Risks and Hedging Analysis" on https://www.isda.org/a/pMWgE/Crypto-asset-Risks-and-Hedging-Analysis.pdf

References

Acerbi, C. (2002): "Spectral measures of risk: A coherent representation of subjective risk aversion," *Journal of Banking & Finance*, 26, 1505–1518.

Akaike, H. (1973): "Information theory and an extension of the maximum likelihood principle," in *Second International Symposium on Information Theory*, ed. by B. N. Petrov and F. Csaki, Budapest: Akadémiai Kiado, 267–281.

Alexander, C., D. F. Heck, and A. Kaeck (2022): "The role of binance in bitcoin volatility transmission," *Applied Mathematical Finance*, 1–32.

Anderson, D., K. Burnham, and G. White (1998): "Comparison of Akaike information criterion and consistent Akaike information criterion for model selection and statistical inference from capture-recapture studies," *Journal of Applied Statistics*, 25, 263–282.

Artzner, P., F. Delbaen, J.-M. Eber, and D. Heath (1999): "Coherent measures of risk," *Mathematical Finance*, 9, 203–228.

Barbi, M. and S. Romagnoli (2014): "A Copula-Based Quantile Risk Measure Approach to Estimate the Optimal Hedge Ratio," *Journal of Futures Markets*, 34, 658–675.

Barndorff-Nielsen, O. E. (1997): "Normal inverse Gaussian distributions and stochastic volatility modelling," *Scandinavian Journal of statistics*, 24, 1–13.

Breymann, W., A. Dias, and P. Embrechts (2003): "Dependence structures for multivariate high-frequency data in finance," .

Cherubini, U., S. Mulinacci, and S. Romagnoli (2011): "A copula-based model of speculative price dynamics in discrete time," *Journal of Multivariate Analysis*, 102, 1047–1063.

Cont, R. (2001): "Empirical properties of asset returns: stylized facts and statistical issues," *Quantitative Finance*, 1, 223–236.

Davison, A. C. and D. V. Hinkley (1997): *Bootstrap methods and their application*, 1, Cambridge university press.

Demarta, S. and A. J. McNeil (2005): "The t copula and related copulas," *International statistical review*, 73, 111–129.

Dowd, K., J. Cotter, and G. Sorwar (2008): "Spectral risk measures: properties and limitations," *Journal of Financial Services Research*, 34, 61–75.

Dungey, M., O. Henry, and L. Hvozdyk (2013): "The impact of jumps and thin trading on realized hedge ratios?" .

Ederington, L. H. (1979): "The hedging performance of the new futures markets," *The journal of finance*, 34, 157–170.

Efron, B. (1979): "Bootstrap methods: another look at the jackknife," *Annals of Statistics*, 1–26.

Efron, B. and R. J. Tibshirani (1994): *An introduction to the bootstrap*, CRC press.

Embrechts, P., A. McNeil, and D. Straumann (2002): "Correlation and dependence in risk management: properties and pitfalls," *Risk management: value at risk and beyond*, 1, 176–223.

Fama, E. F. (1963): "Mandelbrot and the stable Paretian hypothesis," *The Journal of Business*, 36, 420–429.

Fisher, N. I. and P. K. Sen (2012): *The collected works of Wassily Hoeffding*, Springer Science & Business Media.

Föllmer, H. and A. Schied (2002): *Stochastic Finance. An Introduction in Discrete Time*, de Gruyter.

Genest, C. (1987): "Frank's family of bivariate distributions," *Biometrika*, 74, 549–555.

Genest, C., K. Ghoudi, and L.-P. Rivest (1995): "A semiparametric estimation procedure of dependence parameters in multivariate families of distributions," *Biometrika*, 82, 543–552.

Genest, C. and L.-P. Rivest (1993): "Statistical inference procedures for bivariate Archimedean copulas," *Journal of the American statistical Association*, 88, 1034–1043.

Gyamerah, S. A. and C. Abaitey (2022): "Modelling and forecasting the volatility of bitcoin futures: the role of distributional assumption in GARCH models," *Data Science in Finance and Economics*, 2, 345–358.

Härdle, W. K., N. Hautsch, and L. Overbeck (2008): *Applied Quantitative Finance*, Springer Science & Business Media.

Härdle, W. K., M. Müller, S. Sperlich, and A. Werwatz (2004): *Nonparametric and Semiparametric Models*, Springer Science & Business Media.

Härdle, W. K. and O. Okhrin (2010): "De copulis non est disputandum," *AStA Advances in Statistical Analysis*, 94, 1–31.

Härdle, W. K. and L. Simar (2019): *Applied multivariate statistical analysis Fifth Edition*, Springer.

Harris, R. D., J. Shen, and E. Stoja (2010): "The Limits to Minimum-Variance Hedging," *Journal of Business Finance & Accounting*, 37, 737–761.

Hoeffding, W. (1940a): "Masstabinvariante Korrelationstheorie," *Schriften des Mathematischen Instituts und Instituts fur Angewandte Mathematik der Universitat Berlin*, 5, 181–233.

——— (1940b): "Scale-invariant correlation theory (English translation)," 5, 181–233.

——— (1941): "Scale-invariant correlations for discontinuous distributions (English translation)," 7, 49–70.

Hull, J. C. (2003): *Options futures and other derivatives*, Pearson Education India.

Joe, H. (1997): *Multivariate models and multivariate dependence concepts*, CRC Press.

Kaiser, L. (2019): "Seasonality in cryptocurrencies," *Finance Research Letters*, 31.

Kalemanova, A., B. Schmid, and R. Werner (2007): "The normal inverse Gaussian distribution for synthetic CDO pricing," *The Journal of Derivatives*, 14, 80–94.

Katsiampa, P., L. Yarovaya, and D. Zikeba (2022): "High-Frequency connectedness between bitcoin and other top-traded crypto assets during the COVID-19 crisis," *Journal of International Financial Markets, Institutions and Money*, 101578.

Krupskii, P. and H. Joe (2013): "Factor copula models for multivariate data," *Journal of Multivariate Analysis*, 120, 85–101.

Kruskal, W. H. (1958): "Ordinal measures of association," *Journal of the American Statistical Association*, 53, 814–861.

Mark, M., J. Sila, and T. A. Weber (2022): "Quantifying endogeneity of cryptocurrency markets," *The European Journal of Finance*, 28, 784–799.

McNeil, A., R. Frey, and P. Embrechts (2005): *Quantitative Risk Management*, Princeton, NJ: Princeton University Press.

——— (2015): *Quantitative Risk Management*, Princeton, NJ: Princeton University Press, 2nd ed.

Menezes, C., C. Geiss, and J. Tressler (1980): "Increasing downside risk," *The American Economic Review*, 70, 921–932.

Meshcheryakov, A., S. Ivanov, et al. (2020): "Ethereum as a hedge: the intraday analysis," *Economics Bulletin*, 40, 101–108.

Nakamoto, S. (2009): "Bitcoin: A Peer-to-Peer Electronic Cash System," .

Nelsen, R. (2002): "Concordance and copulas: A survey," in *Distributions with Given Marginals and Statistical Modelling*, Kluwer Academic Publishers, 169–178.

Nelsen, R. B. (1999): *An Introduction to Copulas*, Springer.

Petukhina, A. A., R. C. Reule, and W. K. Härdle (2021): "Rise of the machines? Intraday high-frequency trading patterns of cryptocurrencies," *The European Journal of Finance*, 27, 8–30.

Politis, D. N. and J. P. Romano (1994): "The Stationary Bootstrap," *Journal of the American Statistical Association*, 1303–1313.

Schweizer, B., E. F. Wolff, et al. (1981): "On nonparametric measures of dependence for random variables," *Annals of Statistics*, 9, 879–885.

Sheu, H.-J. and Y.-S. Lai (2014): "Incremental value of a futures hedge using realized ranges," *Journal of Futures Markets*, 34, 676–689.

Sklar, A. (1959): "Fonctions de répartition a n dimensions et leurs marges," *Publications de l'Institut de Statistique de l'Universite de Paris*, 8, 229–231.

Takeuchi, K. (1976): "Distribution of informational statistics and a criterion of model fitting. Suri-Kagaku (Mathematical Sciences) 153 12-18," .

Tse, Y. and M. R. Williams (2013): "Does index speculation impact commodity prices? An intraday analysis," *Financial Review*, 48, 365–383.

Zeevi, A. and R. Mashal (2002): "Beyond correlation: Extreme co-movements between financial assets," *Available at SSRN 317122.*

Zhang, L., T. Wu, S. Lahrichi, C.-G. Salas-Flores, and J. Li (2022): "A Data Science Pipeline for Algorithmic Trading: A Comparative Study of Applications for Finance and Cryptoeconomics," in *2022 IEEE International Conference on Blockchain (Blockchain)*, IEEE, 298–303.

A Density of linear combination of random variables

Proposition 6 *Let $\boldsymbol{X} = (X_1, ..., X_d)^\top$ be real-valued random variables with corresponding copula density $\boldsymbol{c}_{X_1,...,X_d}$, and continuous marginals $F_{X_1}, ..., F_{X_d}$. Then, the pdf of the linear combination of marginals $Z = n_1 \cdot X_1 + ... + n_d \cdot X_d$ is*

$$f_Z(z) = \left|n_1^{-1}\right| \int_{[0,1]^{d-1}} \boldsymbol{c}_{X_1,...,X_d}\left(F_{X_1}(S(z)), u_2, ..., u_d\right) \cdot f_{X_1}(S(z)) \mathrm{d}u_2 ... \mathrm{d}u_d, \tag{9}$$

with

$$S(z) = \frac{1}{n_1} \cdot z - \frac{n_2}{n_1} \cdot F_{X_2}^{(-1)}(u_2) - ... - \frac{n_d}{n_1} \cdot F_{X_d}^{(-1)}(u_d).$$

Proof. (delete – already introduced above: Let $Z = n_1 \cdot X_1 + ... + n_d \cdot X_d$ and let) Let $\mathbf{A} = \begin{bmatrix} n_1 & n_2 & \cdots & n_d \\ 0 & 1 & \cdots & 0 \\ \vdots & & \ddots & \vdots \\ 0 & \cdots & & 1 \end{bmatrix}$. *[The specification of the matrix is not clear. How does the row proceed after 1 in the second row, when it ends in 0?]* Then,

$$\begin{bmatrix} Z \\ X_2 \\ \vdots \\ X_d \end{bmatrix} = \boldsymbol{A} \begin{bmatrix} X_1 \\ X_2 \\ \vdots \\ X_d \end{bmatrix}.$$

By transformation of the variables (Härdle and Simar, 2019) *[If you cite a book and have a particular formula or section in mind, then state it.]*

$$\begin{aligned} \boldsymbol{f}_{Z,X_2,...,X_d}(z, x_2, ..., x_d) &= \boldsymbol{f}_{X_1,...,X_d}\left(\boldsymbol{A}^{-1} \begin{bmatrix} z \\ x_2 \\ \vdots \\ x_d \end{bmatrix}\right) \cdot |\det \boldsymbol{A}^{-1}| \\ &= \left|n_1^{-1}\right| \boldsymbol{f}_{X_1,...,X_d}\left(S(z), x_2, ..., x_d\right). \end{aligned}$$

Let $u_i = F_{X_i}(x_i)$ and by chain rule we have

$$\begin{aligned} \boldsymbol{f}_{X_1,...,X_d}(x_1, ..., x_d) &= \frac{\partial^d F_{X_1,...,X_d}(x_1, ..., x_d)}{\partial x_1 ... \partial x_d} \\ &= \boldsymbol{c}_{X_1,...,X_d}(u_1, ..., u_d) \cdot \prod_{i=1}^{d} f_{X_i}(x_i). \end{aligned}$$

Therefore,

$$\begin{aligned} &\boldsymbol{f}_{Z,X_2,...,X_d}(z, x_2, ..., x_d) = \\ &\quad \left|n_1^{-1}\right| \cdot \boldsymbol{c}_{X_1,...,X_d}\left(F_{X_1}(S(z)), u_2, ..., u_d\right) \cdot f_{X_1}\{S(z)\} \cdot \prod_{i=2}^{d} f_{X_i}(x_i). \end{aligned}$$

The claim (9) is obtained by integrating out $x_2, ...x_d$ by substituting $\mathrm{d}x_i = \frac{1}{f_{X_i}(x_i)}\mathrm{d}u_i$. ■

B Summary Statistics of Assets

	Mean %	Std %	Skew	Kurt	MD %	MD date	ρ	τ
Hedging Instrument								
BTCF	0.3906	4.6312	-0.5060	4.4204	-26.9920	2020-03-12	1.0000	1.0000
Individual Cryptos								
BTC	0.3915	4.4023	-0.5857	4.6565	-25.9965	2020-03-12	0.9975	0.9507
ETH	0.6819	6.0103	-0.2557	5.2646	-32.0144	2020-03-12	0.7712	0.5988
ADA	0.9467	6.6990	0.1661	2.3086	-26.8528	2020-03-12	0.6296	0.4825
LTC	0.3227	6.4781	-0.9935	5.3011	-37.5913	2021-05-19	0.8080	0.6113
XRP	0.2987	7.9843	0.5542	12.4882	-52.7652	2020-12-23	0.4510	0.4939
Crypto Indices with BTC Constituent								
BITX	0.4308	4.5676	-0.8842	4.7222	-27.0220	2020-03-12	0.9769	0.8738
CRIX	0.4602	4.5420	-0.7952	4.7549	-27.1385	2020-03-12	0.9799	0.8769
BITW100	0.4683	4.6174	-0.9864	4.9381	-27.2694	2020-03-12	0.9674	0.8537
Crypto Indices without BTC Constituent								
BITW20	0.6249	5.5021	-1.1518	5.2203	-31.0092	2020-03-12	0.7674	0.5883
BITW70	0.6353	5.8155	-1.1171	5.1926	-32.3453	2021-05-19	0.7525	0.5459

Table 5: Summary statistics of assets' daily returns during the out-of-sample period, from 2019-10-21 to 2021-05-27. The first four columns are the first four moments of assets' daily returns. The fifth and sixth columns are the maximum drawdown (MD) and the date of the MD. The last two columns are Pearson's ρs and Kendall's τs between the assets and BTCF.

C Summary Statistics of Hedged Portfolios

	Mean %	Std %	Skew	Kurt	MD %	MD date	Variance
Individual Cryptos							
BTC	0.0215	0.3221	-1.0119	3.1929	-1.4393	2020-11-30	0.0000
ETH	0.2823	3.8741	0.9469	7.1064	-17.7421	2021-05-19	0.0015
ADA	0.5617	5.2722	1.3634	4.4818	-13.8687	2021-01-08	0.0028
LTC	-0.0871	3.9052	-0.3617	7.6239	-28.3029	2021-05-19	0.0018
XRP	-0.0123	7.1537	1.1451	20.0236	-52.5236	2020-12-23	0.0043
Crypto Indices with BTC Constituent							
BITX	0.0561	0.9954	-0.4204	13.2487	-7.7567	2021-05-19	0.0001
CRIX	0.0812	0.9183	-0.0027	14.3136	-7.1025	2021-05-19	0.0001
BITW100	0.0855	1.1986	-1.7440	22.2644	-11.3866	2021-05-19	0.0001
Crypto Indices without BTC Constituent							
BITW20	0.2429	3.5846	-0.3063	4.1622	-21.4680	2021-05-19	0.0013
BITW70	0.2706	3.8838	-0.6490	4.6312	-23.9984	2021-05-19	0.0015

Table 6: Summary statistics of out-of-sample daily returns of hedged portfolios that minimize variance.

	Mean %	Std %	Skew	Kurt	MD %	MD date	VaR 5%
Individual Cryptos							
BTC	0.0253	0.3294	-0.9725	3.4373	-1.5347	2020-11-30	0.0063
ETH	0.3084	3.8944	1.0243	7.4297	-19.1750	2021-05-19	0.0514
ADA	0.5726	5.2204	1.2981	4.2544	-14.6974	2021-05-19	0.0769
LTC	-0.0742	3.9145	-0.3836	7.5384	-28.3672	2021-05-19	0.0622
XRP	0.0208	7.1520	1.1269	19.8930	-52.5667	2020-12-23	0.0683
Crypto Indices with BTC Constituent							
BITX	0.0562	0.9930	-0.3117	12.4780	-7.5639	2021-05-19	0.0128
CRIX	0.0863	0.9151	0.0718	13.7915	-6.9744	2021-05-19	0.0092
BITW100	0.0846	1.1980	-1.6592	21.3725	-11.2582	2021-05-19	0.0164
Crypto Indices without BTC Constituent							
BITW20	0.2728	3.5940	-0.3721	4.4896	-22.0733	2021-05-19	0.0546
BITW70	0.2847	3.9133	-0.6580	4.7874	-24.6513	2021-05-19	0.0626

Table 7: Summary statistics of out-of-sample daily returns of hedged portfolios that minimize VaR 5%.

	Mean %	Std %	Skew	Kurt	MD %	MD date	VaR 1%
Individual Cryptos							
BTC	0.0176	0.3270	-1.0405	3.3742	-1.5689	2020-11-30	0.0134
ETH	0.2977	3.9132	0.9547	7.2414	-18.6061	2021-05-19	0.1026
ADA	0.5562	5.3466	1.1362	3.9334	-15.4795	2021-05-19	0.1106
LTC	-0.0852	4.1503	-0.7234	7.3208	-29.0915	2021-05-19	0.1030
XRP	0.0352	7.1658	1.1582	19.8506	-52.5727	2020-12-23	0.1387
Crypto Indices with BTC Constituent							
BITX	0.0593	1.0178	-0.5331	13.3100	-8.0299	2021-05-19	0.0247
CRIX	0.0738	0.9695	-0.4729	13.6500	-7.0185	2021-05-19	0.0245
BITW100	0.0823	1.2338	-1.9365	23.1938	-11.8752	2021-05-19	0.0347
Crypto Indices without BTC Constituent							
BITW20	0.2499	3.6210	-0.3866	4.3396	-21.6634	2021-05-19	0.0988
BITW70	0.2788	3.9257	-0.7635	5.1288	-24.5294	2021-05-19	0.1147

Table 8: Summary statistics of out-of-sample daily returns of hedged portfolios that minimize VaR 1%.

	Mean %	Std %	Skew	Kurt	MD %	MD date	ES 5%
Individual Cryptos							
BTC	0.0204	0.3234	-1.0150	3.4423	-1.5629	2020-11-30	0.0101
ETH	0.3082	3.8890	1.0119	7.4077	-18.7819	2021-05-19	0.0782
ADA	0.5525	5.2673	1.2557	4.2423	-14.9647	2021-05-19	0.0984
LTC	-0.0808	3.9829	-0.4957	7.2302	-28.4608	2021-05-19	0.0962
XRP	0.0176	7.1533	1.1411	19.9176	-52.5698	2020-12-23	0.1354
Crypto Indices with BTC Constituent							
BITX	0.0591	1.0065	-0.3453	12.1335	-7.6211	2021-05-19	0.0215
CRIX	0.0777	0.9207	0.0164	13.5608	-6.9894	2021-05-19	0.0173
BITW100	0.0848	1.2125	-1.6397	19.7472	-11.1357	2021-05-19	0.0274
Crypto Indices without BTC Constituent							
BITW20	0.2608	3.6115	-0.3555	4.2016	-21.5430	2021-05-19	0.0804
BITW70	0.2785	3.9157	-0.6949	4.8047	-24.3474	2021-05-19	0.0908

Table 9: Summary statistics of out-of-sample daily returns of hedged portfolios that minimize ES 5%.

	Mean %	Std %	Skew	Kurt	MD %	MD date	ES 1%
Individual Cryptos							
BTC	0.0148	0.3476	-0.8354	3.3054	-1.6225	2020-11-30	0.0234
ETH	0.3080	3.8954	0.9840	7.4947	-18.7625	2021-05-19	0.1299
ADA	0.5016	5.4040	1.1008	3.9607	-15.4481	2021-05-19	0.1463
LTC	-0.1029	4.1581	-0.7757	7.4375	-29.1727	2021-05-19	0.1647
XRP	-0.0200	7.2887	1.1121	18.8732	-52.5700	2020-12-23	0.2516
Crypto Indices with BTC Constituent							
BITX	0.0598	1.0312	-0.4410	11.5863	-7.7424	2021-05-19	0.0411
CRIX	0.0835	0.9461	-0.0361	12.4047	-7.0203	2021-05-19	0.0350
BITW100	0.0781	1.2640	-1.9645	21.8836	-11.9263	2021-05-19	0.0593
Crypto Indices without BTC Constituent							
BITW20	0.2538	3.6323	-0.4086	4.4462	-21.9866	2021-05-19	0.1282
BITW70	0.2660	3.9320	-0.7598	5.0050	-24.4764	2021-05-19	0.1535

Table 10: Summary statistics of out-of-sample daily returns of hedged portfolios that minimize ES 1%.

	Mean %	Std %	Skew	Kurt	MD %	MD date	ERM k=10
Individual Cryptos							
BTC	0.0223	0.3221	-1.0008	3.4153	-1.5242	2020-11-30	0.0057
ETH	0.3117	3.8679	1.0345	7.5751	-18.8729	2021-05-19	0.0491
ADA	0.5722	5.3590	1.4203	4.6970	-14.3885	2021-01-08	0.0700
LTC	-0.0512	3.8812	-0.2929	7.7022	-28.0879	2021-05-19	0.0616
XRP	0.0155	7.1579	1.1244	19.8583	-52.5689	2020-12-23	0.0787
Crypto Indices with BTC Constituent							
BITX	0.0590	1.0078	-0.4427	13.0839	-7.8581	2021-05-19	0.0127
CRIX	0.0840	0.9087	0.0488	14.5501	-7.0530	2021-05-19	0.0100
BITW100	0.0853	1.2032	-1.6522	20.5562	-11.1846	2021-05-19	0.0153
Crypto Indices without BTC Constituent							
BITW20	0.2564	3.6009	-0.3446	4.2152	-21.5920	2021-05-19	0.0503
BITW70	0.2818	3.9074	-0.6952	4.8745	-24.5250	2021-05-19	0.0557

Table 11: Summary statistics of out-of-sample daily returns of hedged portfolios that minimize ERM $k = 10$.

D Supplementary Material: Intraday Hedging

[This section must be shortened significantly. It is not necessary to repeat everything, just point out the differences.]

This supplementary material extends the study in the main body to an intraday rebalancing setting. *[Do we really have intraay rebalancing? Or just intraday P&L? If rebalancing, then clarify.]* The idea is to infer if the findings from the daily setting extend to intraday data or if there are significant differences. Contrary to the setting with with daily data, this requires that we use data from unregulated exchanges.

[From my point of view there is no need to motivate intraday risk management.] Studying the intraday hedge is familiar to academia, e.g. Harris et al. (2010), Dungey et al. (2013), Tse and Williams (2013), and Sheu and Lai (2014).

Numerous studies on the crypto market are associated with or motivated by the presence of intraday traders as well, e.g. Petukhina et al. (2021), Meshcheryakov et al. (2020), Alexander et al. (2022), Zhang et al. (2022) and Katsiampa et al. (2022).

(delete: We have in view to robustify the results from the main body.) The methodology in this supplementary material is similar to the main body, except we

1. form two hedging portfolios, BTC-BTCF and ETH-BTCF,
2. simulate trades using Deribit hourly data, and
3. rebalance every four hours.

D.1 Data

The intraday analysis is built upon a dataset of date range from 2020-06-01 00:00 UTC to 2020-08-01 00:00 UTC. All the price data are sampled hourly. The Deribit contract BTC-25SEP20 (was: 20BTCUSD25SEP20) represents the BTCF; the Deribit BTC and ETH index represent the spot of BTC and ETH, respectively. We take the hourly closing mid-price of the BTCUSD25SEP20 as the futures price and the last value of the BTC and ETH index in every hourly bucket as the spot prices. Since the date range of the data is fully covered by the lifetime of BTCUSD25SEP20, this study does not require rolling procedure to roll over futures contract near expiry.

D.1.1 Procedure

Starting from oldest data:

1. Calibrate a copula by a training data of 336 datapoints, equivalent to 14 days data
2. Draw samples $(\tilde{r}_s, \tilde{r}_f)$ from the calibrated copula
3. Numerically search for $h^* = \arg\max \phi(\tilde{r}_s - h\tilde{r}_f)$ according to a risk measure ϕ
4. Apply h^* to testing data to yield r_h; the testing data is the consecutive 4 data points to training data, i.e. the 4 hours data consecutive to the last training data
5. Repeat the procedure for the next 4 datapoints
6. Concatenate r_hs the and sort chronologically to form a full length out-of-sample hedging portfolio returns

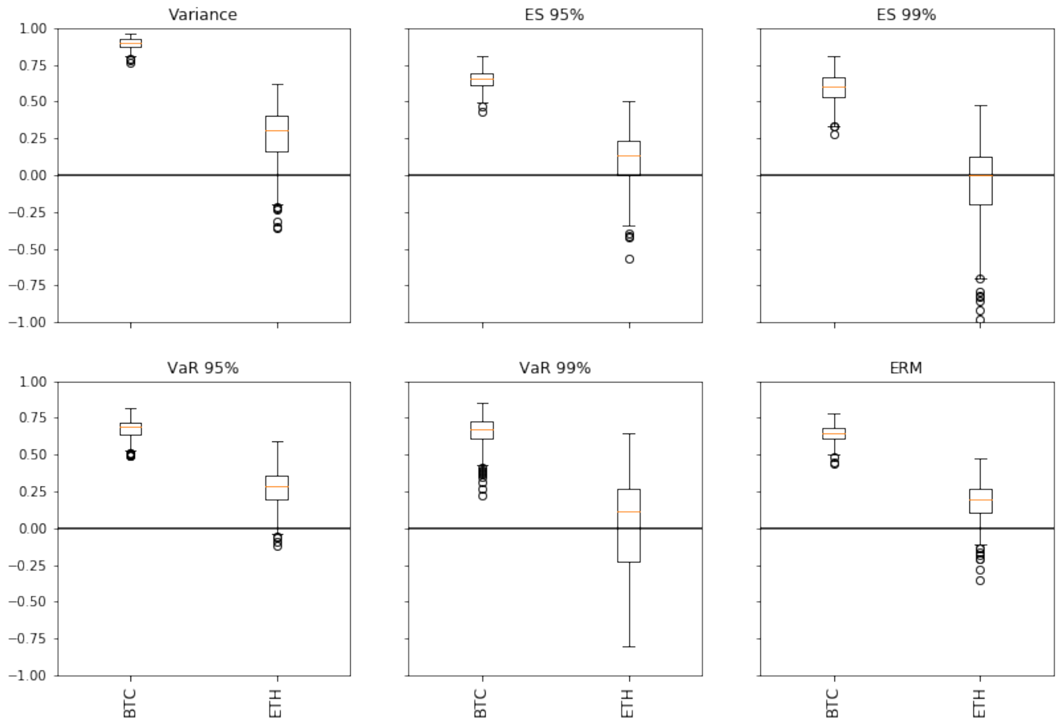

Figure 13: Intraday HEs of BTC-BTCF and ETH-BTCF portfolio. The HEs of BTC-BTCF portfolios are significantly higher than 0, which suggests involving the BTCF in the portfolio can effectively reduce market risk. The HEs of ETH-BTCF portfolios are lower than that of BTC-BTCF portfolios, and sometimes go below 0. We nullify the hedging ability of BTCF in this intraday ETH-BTCF setting.

The procedure is further repeated for all the combinations of risk measures and copulae. The full-length out-of-sample returns represent the corresponding performance of a particular risk measure-copula combination. They are used in computation mean square error (MSE) and lower-semi-variance (LSV) shown in the following section.

The AIC selection step is performed between Steps 1 and 2 of the procedure above. The resulting out-of-sample returns are a mix of results from the copula that has the lowest AIC on the training data. We keep a record of how many times a copula is choosen by this step. To yield robust HE measures, we apply stationary bootstrapping to the full-length AIC selected out-of-sample returns with the following parameters: $p = 1/4, T = 300, N = 1000$.

D.2 Results

Bootstrapped out-of-sample HEs: The analysis begins with the boxplot in figure 13 of the bootstrapped out-of-sample HEs. In general, most of the daily rebalancing results of BTC-BTCF carry over to the intraday rebalancing schedule; *[This can be* **significantly** *shortened!]* The intraday rebalancing ETH-BTCF is different from its daily rebalancing counterpart. Note that the exact values of HEs from the two rebalancing schedules should not be directly compared for two reasons: 1. The data are from different date ranges; 2. Various factors contribute to the difference between results from different sampling frequencies, e.g. Epps effect, microstructure noise, and asynchronous trading. However, we compare the patterns and conclusions to get a general understanding of the hedging issue

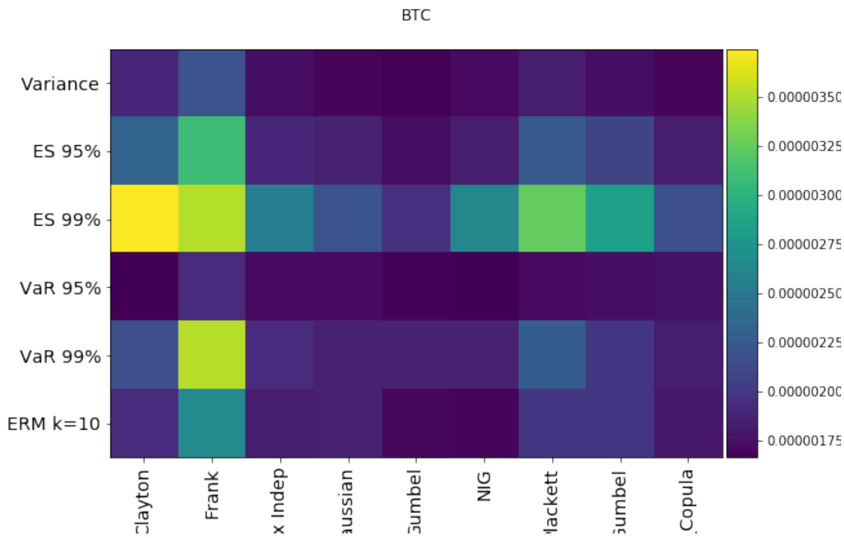

Figure 14: Intraday out-of-sample MSEs of the BTC-BTCF portfolio constructed by combinations of copula and ris minimization objectives. The Frank copula is again inferior. Minimising ES99% results in higher MSEs disregard of which copula is in use. *[Graph is cut off. Make pdf or eps.]*

for future use.

The main difference between the intraday rebalancing and daily rebalancing ETH-BTCF portfolio is that negative HEs appear in the intraday results in all the risk measures we consider. This implies that hedgers cannot draw on potential intraday dependence between BTC and ETH to hedge an ETH crypto position. (delete: The negative HEs suggests that BTCF should not be used to hedge against ETH in an intraday setting. Consider also the fact that BTCF is written on BTC instead of ETH, hedgers have no ground to assume they can take advantage of the intraday dependency structure between ETH and BTCF for hedging. Therefore, we mainly focus on the BTC-BTCF portfolios and mentioning the results of the ETH-BTCF portfolio is needed.)

Turning to BTC-BTCF, among the (delete: *BTC-BTCF HEs*: The HEs of BTC-BTCF are significantly higher than zero across different risk measures, suggesting that adding BTCF to a BTC portfolio can effectively reduce the risk measured by selected measures. Among) risk measures, HE of variance is the highest (delete: for the BTC-BTCF portfolio), ranging between 72% to 98%, while the HE's other risk measures range between 25% to 80%. The finding that reducing variance is a well-achievable objective is consisten with the findings of the daily rebalancing schedule. *[We can consider deleting the discussion about 99% risk measures...]* On the other hand, the HEs of ES99% and VaR99% are relatively more dispersed and skewed to the left. Both risk measures consider only 1% of the data from the left for deciding the hedge ratio and computing the HEs. Considering only a few data points naturally leads to a less reliable hedge ratio and lower consistency HEs. Evidence also shows that ES99% VaR99% minimising portfolios have higher MSE and LSV. This result is again consistent with the daily rebalancing setting.

Figures 14 and 15 report the out-of-sample MSE and LSV of the BTC-BTCF when different copulae and risk measures are in use. The MSE and LSV are in a similar magnitude *[than what?]* with a few exceptions, a similar pattern to the daily rebalancing setting. *[Fix sentence.]*

Across various copulae, the BTC-BTCF portfolio that minimises VaR95% provides the lowest MSE and LSV. Portfolios that minimise variance and ERM with $k = 10$ result in similar magnitudes

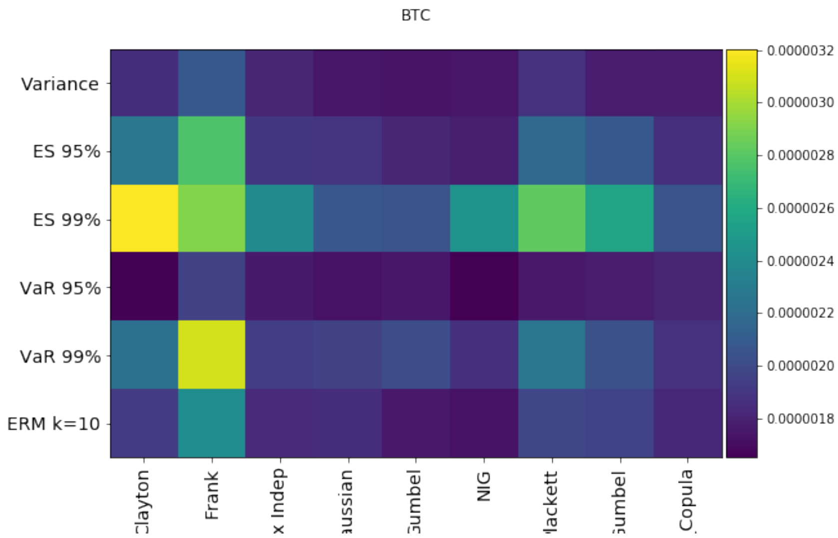

Figure 15: Intraday out-of-sample LSVs of the BTC-BTCF portfolio constructed by combinations of copula and ris minimization objectives. The Frank copula is again inferior. Minimising ES99% results in higher MSEs disregard of which copula is in use.

Spot/ Copula	t	Plackett	GMI	rotGumbel	NIG
BTC	60.00	1.11	3.33	8.89	26.67
ETH	35.14	0	24.32	15.68	24.86

Table 12: Intraday copula selection results (shortened). The values are the percentage counts of a copula chosen by the AIC procedure during the out-of-sample period. The table shows only the frequently chosen copula, i.e. t, Plackett, Gaussian Mix Independent (GMI), rotated Gumbel (rotGumbel), and Normal Inverse Gaussian factor copula (NIG).

of MSEs and LSVs *[than what?]*, which are slightly greater than VaR95%, especially when Gumbel and NIG copulae are in use to model the dependence. ES99% generates the highest MSEs and LSVs, regardless of the copula. (delete: Notice that the portfolios that minimise ES99% and VaR99% are generally riskier than their 95% counterparts in terms of MSEs and LSVs.)

Across various risk measures, Gumbel and NIG copulae perform well in the resulting portfolios' MSE and LSV, except for ES99%. The Frank copula performs worst, regardless of the risk measure. These results are consistent with the daily rebalancing setting and results in other literature. *[Other literature? Perhaps better to delete this. Or be more specific.]* As Gumbel and NIG are the only copulae that can model upper tail dependence, this suggests that the upper tail dependence is an essential feature of the dependence structure for hedging. *[Delete?]* The conclusion is further supported by comparing the Gumbel and the rotated Gumbel copula. The rotated Gumbel copula is the 180-degree rotated version of the Gumbel copula, sharing all the features of the Gumbel copula but switching from modelling the lower tail dependence to upper tail dependence. The rotated Gumbel copula results in portfolios with higher MSEs and LSVs consistently across risk measures.

Table 12 shows the relative frequencies of the best fitting copula according to AIC.

[No need to repeat all the numbers in the text, as they are given in the table. Draw conclusions directly and mention only exceptional numbers.] They are t-, Plackett, Gaussian Mix Independent,

rotated Gumbel and NIG. Similar to the result in the daily rebalancing schedule, most of the time, 60% in this case, the AIC procedure chooses t-Copula to model the dependence structure of BTC-BTCF in the intraday setting. For the rest of the time, the NIG copula is mainly chosen, accounting for around 26% of the time. Rotated Gumbel, Gaussian Mix Independent, and Plackett are spontaneously chosen. On the other hand, the intraday ETH-BTCF's AIC selection result is very different from that of the daily rebalancing. There are three copulae: t-, Gaussian Mix Independent, and NIG copula, that are closely chosen, instead of a single copula, rotated Gumbel copula, dominating the list in the daily rebalancing setting. In the intraday setting, the three copulae are chosen 35.1%, 24.9%, and 24.3% of the time, respectively.